Historic England

Scientific Dating

St Giles House and the 'Riding House', Wimborne St Giles, Dorset

Scientific Dating and Bayesian Chronological Modelling

Ian Bailiff, Alex Bayliss, Martin Bridge, Christopher Bronk Ramsey, John Cattell, Elaine Dunbar, and Cathy Tyers

Discovery, Innovation and Science in the Historic Environment

Research Report Series no. 69-2017

Front Cover: St Giles House view from the E (© Historic England, DP167048; photograph by James Davies)

ST GILES HOUSE AND THE 'RIDING HOUSE' WIMBORNE ST GILES, DORSET

Scientific Dating and Bayesian Chronological Modelling

Ian Bailiff, Alex Bayliss, Martin Bridge, Christopher Bronk Ramsey, John Cattell, Elaine Dunbar, and Cathy Tyers

NGR: SU 03236 11591 and SU 03305 11698

ISSN 2398-3841 (Print)
ISSN 2059-4453 (Online)

SUMMARY
An interdisciplinary study involving documentary research and investigation of the fabric of St Giles House was undertaken between 2003 and 2017. The detailed understanding gained has underpinned a detailed programme of repairs and conservation works. As part of a pilot study to determine the feasibility of using luminescence dating of brick to understand historic buildings, 15 bricks were sampled and analysed in 2003–5. In 2014, 15 timbers were sampled for dendrochronology from six areas of the building, and subsequently radiocarbon dating and wiggle-matching was undertaken on two of these cores which could not be dated by dendrochronology. Bayesian chronological modelling was undertaken to combine the scientific dates with the relative and absolute dating of the surviving fabric known from architectural, structural, and documentary evidence.

This analysis has clarified the extent of the documented constructed phases. Luminescence dates from the basement show that the east addition of AD 1650–9 incorporated some fragments of an earlier manor house on the site together with some rebuilding. A mid sixteenth-century doorway in this area is reset in a later section of walling. Another luminescence date and the date for a wiggle-matched timber show that this campaign also extended a little further west than previously supposed, including both the north wall and the ceiling beams of what may in the mid-sixteenth century have formed a ground-floor entrance hall. The section containing the putative entrance hall and the great dining room, above, probably slightly predates the AD 1650–9 east addition. Work in AD 1670–4 extended slightly further west and north than thought previously, with works to both the upper brickwork in the Southampton Room being attested by luminescence dating and re-roofing of the Handel Room demonstrated by dendrochronology.

Dendrochronology has also shown that the roof over the Southampton Room in the White Hall range was replaced in winter AD 1734/35 or shortly thereafter. Most elements of the surviving fabric that were thought to pre-date AD 1650 have been assigned by the scientific dating and structural phasing to later building campaigns. Luminescence dating and structural phases, however, combine to suggest that the White Hall range was built in *AD 1633–1650 (95% probability)*, probably in *AD 1643–1650 (68% probability)*. Most likely this occurred in AD 1639 or shortly after, when Sir Anthony Ashley-Cooper came of age and took possession of his house from the Court of Wards. A timber dated by radiocarbon wiggle-matching from a lintel over the fireplace in the same area of walling was reused.

Eleven timbers from the ‘Riding House’, which was almost certainly built as stables, were also sampled for dendrochronology, those from the roof being successfully dated and yielding felling dates in summer AD 1615 and summer AD 1616.

CONTRIBUTORS

Ian Bailiff, Alex Bayliss, Martin Bridge, Christopher Bronk Ramsey, John Cattell, Elaine Dunbar, and Cathy Tyers

ACKNOWLEDGEMENTS

We are grateful to the owner, the Earl of Shaftesbury, who made us welcome during the various site visits, and to Philip Hughes (Philip Hughes Associates) who facilitated those visits, provided assistance throughout the investigation, and supplied plans of the buildings for use in this report. Thanks are also due to Richard Bond, Rebecca Child, and Rebecca Lane for assistance with sampling, and to Shahina Farid and Derek Hamilton for commissioning and enabling these analyses. Shahina Farid undertook the statistical simulations which determined the sampling strategy for radiocarbon wiggle-matching. Figures 6–8 and 11–13 were greatly improved by Andy Crispe, and the cover photograph was taken by James Davies.

ARCHIVE LOCATION

Dorset Historic Environment Record
Environment and the Economy
Dorset County Council
County Hall
Colliton Park
Dorchester
Dorset DT1 1XJ

DATE OF RESEARCH

2003–17

CONTACT DETAILS

Ian Bailiff
Luminescence Dating Laboratory
Department of Archaeology
University of Durham
South Road
Durham DH1 3LE

Alex Bayliss and Cathy Tyers
Historic England
Fourth Floor
Cannon Bridge House
25 Dowgate Hill
London EC4R 2YA
alex.bayliss@historicengland.org.uk
cathy.tyers@historicengland.org.uk

Martin Bridge
UCL Institute of Archaeology
31–34 Gordon Square
London WC1H 0PY
martin.bridge@ucl.ac.uk

Christopher Bronk Ramsey
Oxford Radiocarbon Accelerator Unit
Research Laboratory for Archaeology
Dyson Perrins Building
South Parks Road
Oxford OX1 3QY
christopher.ramsey@rlaha.ox.ac.uk

John Cattell
Historic England
The Engine House
Fire Fly Avenue
Swindon SN2 2EH
john.cattell@historicengland.org.uk

Elaine Dunbar
SUERC Radiocarbon Laboratory
Scottish Enterprise Technology Park
Rankine Avenue
East Kilbride G75 1QF
elaine.dunbar@glasgow.ac.uk

CONTENTS

INTRODUCTION

St Giles House (Fig 1) is a Grade I listed country house that was placed on the Buildings at Risk Register (now the Heritage at Risk Register) in 1998. However, following major restoration works, undertaken by the twelfth Earl of Shaftesbury, St Giles House was removed from the register in 2015. It is situated in extensive grounds in East Dorset, just south of Cranborne Chase, and close to the Hampshire and Wiltshire borders (Figs 2–4).

The construction of the main body of the brick-built house is thought to be seventeenth century, although it potentially incorporates earlier phases in the basement. The earliest fabric probably formed part of an earlier manor house on the site dating from the late-fifteenth or early sixteenth century; a full account being available in Cattell and Barson (2003). Extensive additions and alterations were made in the mid-eighteenth century by Henry Flitcroft (1740–4), with further modifications and additions made in the nineteenth century (1813–20 and 1854). The 1970s saw the house abandoned as a family home, resulting in it becoming partly derelict until the twelfth Earl of Shaftesbury inherited. Although the sequence of the different phases of construction in the west, north, and east ranges has been established on the basis of structural and architectural analysis, their dates of construction are less well understood.

Luminescence dating was initiated in 2003 as part of the measured survey, structural analysis, and documentary history that was undertaken on St Giles House at that time to inform the anticipated programme of repairs. This was a pilot study to determine the feasibility of using luminescence dating of brick to understand historic buildings, as this technique had not previously been applied to such a purpose in the UK. St Giles House was chosen as the complex sequence of structural phases, many of which could be dated by reference to documentary sources, could validate the results produced.

Dendrochronology was requested by John Cattell (HE Head of Investigation and Analysis) in 2014 in order to establish dates for the earliest parts of the building, and to provide dating evidence for some subsequent phases of construction. In 2015, radiocarbon wiggle-matching was undertaken on two tree-ring sequences from the earliest structural phases which could not be dated by dendrochronology.

The so-called 'Riding House' (Fig 5), which was almost certainly built as stables, is situated north-east of the main house (Fig 4) and was also in a neglected state. It lies on the southern side of the home farm complex and is a Grade II* listed building. It is a two-storey brick building with stone dressings and a tiled roof. It was thought to date to the first quarter of the seventeenth century with its construction attributed on stylistic grounds to Sir Anthony Ashley (Cattell and Barson 2003; Lane 2016). The south elevation, that is the main facade, is of nine bays, with the four wide bays being gabled and the five narrower bays having eaves. The roof has eight chamfered tiebeam trusses with collars and queen-struts that support the two chamfered purlins on each side (RCHME 1975; Lane 2016).

Dendrochronological dating of the 'Riding House' was requested by Francis Kelly (HE Inspector of Historic Buildings and Areas) in relation to listed building consents associated with the planned renovation and refurbishment for sustainable reuse and to inform the building investigation undertaken by Rebecca Lane of the HE Assessment Team.

DENDROCHRONOLOGY

Dendrochronological assessment and sampling were undertaken in the latter half of 2014. In the initial assessment of dendrochronological potential, accessible oak timbers with more than 50 rings and where possible traces of sapwood were sought, although slightly shorter sequences are sometimes sampled if little other material is available. Those timbers judged to be potentially useful were subsequently cored using a 15mm auger attached to an electric drill. The cores were glued to wooden laths, labelled, and stored for subsequent analysis.

Methodology

Standard dendrochronological methodological approaches were employed (see eg English Heritage 1998). The cores were polished on a belt sander using 80 to 400 grit abrasive paper to allow the ring boundaries to be clearly distinguished. The samples had their tree-ring sequences measured to an accuracy of 0.01mm, using a specially constructed system utilising a binocular microscope with the sample mounted on a travelling stage with a linear transducer linked to a PC, which recorded the ring widths into a dataset. The software used in measuring and subsequent analysis was written by Ian Tyers (2004). Cross-matching was attempted by a combination of visual matching and a process of qualified statistical comparison by computer. The ring-width series were compared for statistical cross-matching, using a variant of the Belfast CROS program (Baillie and Pilcher 1973). Ring sequences were plotted on the computer monitor to allow visual comparisons to be made between sequences. This method provides a measure of quality control in identifying any potential errors in the measurements when the samples cross-match.

In comparing one sample or site master against other samples or chronologies, *t*-values over 3.5 are considered significant, although in reality it is common to find demonstrably spurious *t*-values of 4 and 5 because more than one matching position is indicated. For this reason, dendrochronologists prefer to see some *t*-value ranges of 5, 6, and higher, and for these to be well replicated from different, independent reference chronologies with both local and regional chronologies well represented, except where imported timbers are identified. Where two individual samples match together with a *t*-value of 10, or above, and visually exhibit exceptionally similar ring patterns, they may have originated from the same parent tree. Same-tree derivation can also be identified through the external characteristics of the timber itself, such as knots and shake patterns. Lower *t*-values, however, do not preclude same-tree derivation.

Ascribing felling dates and date ranges

Once a tree-ring sequence has been firmly dated in time, a felling date, or date range, is ascribed where possible. With samples which have sapwood complete to the underside of, or including bark, this process is relatively straightforward. Depending on the completeness of the final ring (ie if it has only the spring vessels or early wood formed, or the latewood or summer growth) a precise felling date and season can be given. If the sapwood is partially missing, or if only a heartwood/sapwood transition boundary survives, then an estimated felling date range can be given for each sample. The number of sapwood rings can be estimated by using an empirically derived sapwood estimate with a given confidence limit. If no sapwood or heartwood/sapwood boundary survives then the minimum number of sapwood rings from the appropriate sapwood estimate is added to the last measured ring to give a *terminus post quem* for felling (a felled-after date).

A review of the geographical distribution of dated sapwood data from historic timbers has shown that a sapwood estimate relevant to the region of origin should be used in interpretation, which in this area is 9–41 rings (Miles 1997). It must be emphasised that dendrochronology can only date when a tree has been felled, not when the timber was used to construct the structure or object under study.

Results

St Giles House

A series of areas that were considered key with respect to enhancing the overall understanding of the development of St Giles House were initially assessed for dendrochronological potential. However, the first-floor frames of the east and north ranges were found to be inaccessible following re-flooring work and the second-floor frame of the north range was found to contain large fast-grown timbers, including one large softwood beam, with too few rings for successful analysis. In spite of other areas of interest containing only few timbers considered to have dendrochronological potential the decision was made, following discussion, to proceed with sampling. The areas sampled were: in the basement; the Hall (the former 'putative' entrance hallway), in the north range; the Pantry (formerly the 'bathing room') in the south range; and the Butler's Pantry in the west range (Fig 6), the east range attics (Fig 7), and the roofs in the west range over the Handel Room and Southampton Room (Fig 8). The extent of the sampling was limited due to the overall unsuitable nature of many of the timbers, with a total of only 16 timbers being sampled (Table 1a).

The samples from two timbers (wsgh03 and wsgh06) proved to have insufficient rings for reliable analysis and hence were excluded from further analysis. Duplicate samples were taken from the west range fireplace lintel in the Butler's Pantry (wsgh16), in order to maximise the ring sequence. These were both measured in spite of having less than 40 rings but could not be cross-matched to produce a combined sequence of sufficient length for reliable analysis. All other measured series were compared. Four series from the roof over the Handel Room were successfully cross-matched (Table 2a), as were two series from the roof over the Southampton Room (Table 2b). These matched series were combined to produce a site master chronology, WSGHHRR, of 119-years representing the Handel Room roof (Fig 10) and a site master chronology, WSGH1415, of 79-years representing the roof over the Southampton Room (Fig 10). These two site masters were compared with an extensive range of reference chronologies and were both successfully dated (Tables 3a and 3b). The remaining unmatched cores were also compared to an extensive range of reference chronologies but none were successfully dated.

The 'Riding House'

The initial assessment of dendrochronological potential established that those timbers accessible at ground-floor level (eg ceiling beams and lintels) were derived from fast-grown timbers with too few rings for successful analysis. However, those timbers associated with the roof were assessed as suitable for analysis. Access to the roof trusses was again limited, with the three easternmost trusses being fully exposed, the fourth partially obscured and only tiebeams and some principal rafter feet being accessible on other trusses, except for the westernmost truss where there is no tiebeam but the principal rafters and purlins were accessible. Thus, sampling was restricted and less extensive than would usually be undertaken on a structure of this size. Ten samples were taken from timbers associated with the roof and a further sample was taken from a vertical post on the stairs which was considered of key importance as it was suspected as possibly being from an earlier structure (probably a decorative arcade), although it was heavily paint covered, and, hence not possible to assess for suitability (Table 1b and Fig 9). The latter sample proved to have too few rings for analysis.

The ten measured series from the roof timbers were compared. Seven series were found to cross-match each other (Table 2c) and were combined to produce a 205-year site chronology, WSGRIDHO (Fig 10), which was subsequently dated (Table 3c). The remaining three series, notably the three shortest series obtained from the roof, failed to give satisfactory cross-matches with the dated roof series and could not be dated individually when compared to an extensive range of reference chronologies.

Interpretation and discussion

St Giles House

No samples were successfully dated from timbers from the south-range basement floor, north range, west range, or from the east-range attic floor. However, four timbers, three principal rafters and a purlin, in the roof over the Handel Room were dated and appear likely to be coeval (Table 3a and Fig 10). The mean heartwood-sapwood boundary date was AD 1641, giving a likely felling date range for the group of AD 1659–82, allowing for rings present on wsgh12. This indicates that these timbers were used in the construction of this roof around the middle of the second half of the seventeenth century. The dating evidence (Table 3a) for this group of timbers suggests that they were likely to have been derived from relatively locally grown trees.

Two timbers, a strut and a brace, from the king-post roof over the Southampton Room were dated (Table 3b and Fig 10). These two timbers appear likely to be coeval and one of the samples had retained complete sapwood giving a felling date for this pair of timbers of winter AD 1734/35. This indicates that these timbers were used in the construction of this roof shortly after felling in the mid AD 1730s. Again the dating evidence (Table 3b) suggests that the timbers are likely to have been locally sourced.

The dendrochronological analysis, thus, provides evidence for two periods of constructional activity in the west range, one in the latter half of the seventeenth century and one in the first half of the eighteenth century.

The 'Riding House'

All seven of the dated timbers from the roof structure appear to form a coherent group, most likely felled within a short period (Table 3c and Fig 10). Three samples had retained bark edge, two of which were found to have come from trees felled in the summer AD 1615, and one in the summer AD 1616. Thus, construction of the roof is most likely to be in AD 1616, or within a year or two after this latest felling date, therefore, supporting the early seventeenth-century date postulated on architectural and documentary dating evidence. The dating evidence (Table 3c), once again, suggests that the trees used were likely to have been grown locally.

LUMINESCENCE DATING

The luminescence method can be used to date a range of heated archaeological artefacts and deposits such as pottery, brick, flint, and burnt clay and also unheated sediments deposited under suitable conditions. The luminescence chronometer mechanism employs the accumulation and storage of electric charge that has become trapped at special sites in crystals, and luminescence dating is consequently referred to as a trapped charge dating method (Aitken 1985; Duller 2008).

The electric charge becomes available for trapping by the passage of ionising radiation (ie α, β, or γ rays) through crystals such as quartz and feldspar contained in dating samples. When any material is exposed to ionising radiation some of the energy is transferred to the material, causing the material to receive an absorbed dose. If luminescent crystals (such as quartz) are located within the material (eg ceramic) the absorbed dose can be quantified. Radiation causes ionisation of atoms in the material and generates free electrons which diffuse through the material until they become attracted and captured at other locations in the crystal called traps. Electrons can be released from these traps in the laboratory either by heating the material (thermoluminescence, TL) or by the action of light (optically stimulated luminescence, OSL) causing the charge to move to other locations in the crystal where light is emitted as luminescence. The intensity of the luminescence is proportional to the total absorbed dose received since the crystal(s) were last heated to high temperatures (or exposed to bright light). The firing of brick, for example, empties all the traps and the accumulation of trapped charge in the crystals resumes (following cooling) and continues until the next heating, or exposure to light. In the case of brick the luminescent grains within the body of the ceramic are shielded from light by the clay fabric. In laboratory testing the grains are extracted and the cumulative trapped charge can be released by stimulating the grains, either by heating or by light, which causes the release of luminescence. In these experiments the preferred mineral type was quartz, and grains within the size range 90–150μm, referred to as coarse grains, were extracted for measurement.

In the case of fired clay brick (FCB), the luminescent crystals within the clay fabric are located within a radiation 'field' due to radiation emitted during the decay of naturally occurring radioactive isotopes (radioisotopes) of uranium, thorium, and potassium that are naturally present in low concentrations in many environmental materials, in particular rock, clays, sediment, and soil. Because the half-lives of these radioisotopes are extremely long (billions of years) the intensity of the radiation field in the burial medium is essentially constant over archaeological timescales. The intensity of the radiation field is measured in terms of 'dose rate'.

Between the events of the firing of clay to form a ceramic and sample extraction, followed by testing, the luminescent crystals accumulate an absorbed dose (referred to as the paleodose, P), the size of which depends on the length of time between the two events and the quantity of the radioactive isotopes within the fabric and the surrounding medium. The paleodose is determined in the laboratory by measuring the luminescence emitted by crystals extracted from the dating sample and comparing it with the luminescence measured following the administration of a known absorbed dose using a calibrated radiation source. This experimentation can be performed using procedures based on the measurement of either TL or OSL. The dose rate is determined by measuring the radioactivity of the sample (eg the ceramic fabric) and materials within the surrounding environment, since radiation emitted from the radioisotopes within it (within a metre from the sample) can penetrate grains within the sample. The moisture content of the sample and burial medium also affects the dose rate (acting as a radiation moderator) and an average value during burial is estimated. For bricks within a standing structure above ground level this value is generally low (below 5% by weight).

The luminescence age is obtained by evaluating the age equation:

$$\text{Luminescence Age} = \frac{\text{Paleodose}}{\text{Dose rate}} \quad \text{(years)}$$

The luminescence age corresponds to the time elapsed since last heating (firing of clay) and it is an absolute age which does not require a secondary calibration procedure. The evaluation of the age equation was achieved by i) extracting quartz grains within a selected size range from brick core samples and applying a procedure based on the quartz inclusion technique (Aitken 1985) to determine the paleodose, and ii) applying a combination of direct and indirect measurement techniques with samples of the brick, together with other data, to determine the dose rate, as discussed in more detail in the following sections.

Sampling

The building was visited on 18 and 19 August 2003 and potential sampling locations, identified by Richard Bond and Rebecca Child of English Heritage, were inspected under the guidance of Richard Bond. Unfortunately, a high proportion of the walls at the 13 targeted locations had been extensively treated in the late 1980s against dry-rot by drilling and subsequent fluid impregnation with pentachlorophenol (PEN). The PEN, in the form of crystallised deposits within the pore structure of brick and mortar and on the surfaces of walls below the uppermost line of drilling, is highly toxic if inhaled or deposited on the skin if disturbed by drilling and dispersed in the form of an aerosol. This significantly reduced the number of locations that could be cored, and a modified sampling plan was agreed, a summary of which is given below. The locations of the samples are indicated on Figures 11–13, and photographs of the sampling positions are provided in Figures 14–24.

Summary of sample associated with each location:

WSG-01	N-facing external wall of the N range W of 1740s doorway, principal-floor level (Figs 12 and 14a-c)
WSG-02	N-facing external wall of the 1650–9 E addition, principal-floor level (Figs 12 and 14c-e)
WSG-03	S-facing external wall of the 1650–9 E addition, principal-floor level (Figs 12 and 15a-b)
WSG-04	E-facing external wall of the small dining room, principal-floor level (Figs 12 and 16a-b)
WSG-05	W-facing internal wall of engine room in basement (Figs 11 and 17)
WSG-06	N-facing internal wall forming E side of fireplace in Butler’s Pantry (kitchen), basement level (pre-1650–9; Figs 11 and 18a-b)
WSG-07	N-facing internal wall of strong room, basement level (1810–15; Figs 11 and 19a-b)
WSG-08	SW inner corner of stair landing adjoining the first Ivy Room, bedchamber-floor level (Figs 13 and 20)

WSG-09 S-facing external wall of SW block, basement level (1732–49; Figs 11 and 21a-c)

WSG-10 N-facing internal section of the S wall of the Southampton Room, above the White Hall (Figs 13 and 22a-c)

WSG-11 W-facing internal wall near NE corner of strong room, basement level (1810–15; Figs 11 and 23a-b)

WSG-12 E-facing internal wall above NW doorway in basement room at NW corner of 1650–9 E addition (Figs 11 and 24a-b)

Cores of *c* 50mm diameter were cut using a diamond core-drill at twelve locations (WSG-01–WSG-12). At three locations (WSG-01, WSG-02, and WSG-07), two cores were taken to test the suitability of what appeared to be bricks fired at relatively high and low temperatures. At each location a separate 10mm diameter hole was drilled to allow a dosemeter capsule to be placed at a depth of *c* 10cm from the front surface of the wall, and an example of the location of the dosemeters is indicated by a flagged stick in Figure 14b. The dosemeters were collected on 29 March 2004, when three further brick core samples were obtained (WSG-10, WSG-11, and WSG-12).

Methodology

The luminescence age, A, can be expressed by the equation (Aitken 1985):

$$A = \frac{P}{\dot{D}_{tot}} \pm \sigma_{A;} \pm \sigma_B, \qquad (1)$$

where P is the paleodose and $\dot{D}_{tot}$ is the dose rate due to all natural sources of radiation. It is common practice in luminescence dating (Aitken 1989) to calculate two error terms based on the propagation of errors and given at the 68% level of confidence. The first error term, σ_A, is a type A standard uncertainty (ISO 2004) obtained by an analysis of repeated observations (ie random error) and the second error term, σ_B, is a type B standard uncertainty based on an assessment of uncertainty associated with all the quantities employed in the calculation of the age, including those of type A (ie random and systematic errors). The first term is used when comparing luminescence dates from the same site (or by the same laboratory) and the second term (also referred to as the overall error) when making comparisons with independent dating evidence, such as historical records.

Paleodose

Three potentially suitable experimental procedures are available to determine the paleodose: using fine grains (eg 4–1μm) or quartz coarse grains (eg 90–150μm). They are based on the measurement of the 110 °C TL peak (pre-dose), the 210 °C

TL peak, and OSL where the form of the extracted sample can be either as fine or coarse grains. For the dating measurements discussed in this report quartz coarse grains (90–150μm or 150–200μm) were the preferred sample type, and measurements of both OSL and TL (210 °C) were performed using a regenerative procedure (Aitken 1998). Initial tests with quartz coarse grains extracted from the Wimborne St Giles bricks indicated that the OSL signals were significantly stronger than those for the 210 °C TL peak, and hence OSL procedures were used to determine the paleodose.

Measurements with fine-grain samples were not performed. In terms of the dosimetry, fine-grains have a technical advantage over coarse grains since the proportion of the paleodose due to radionuclide sources of lithogenic origin located within the sampled brick core is maximised. Also, the occurrence of anomalous fading in feldspars extracted from fired clay remains a concern and, although the proportion of fine-grain quartz can be increased by the application of a fluorosilicic acid treatment (Berger *et al* 1980), it is not routine and an additional study would be required to apply the full procedure.

Dose rate

The dose rate due to natural sources of radiation, $\dot{D}_{tot}$, was determined by calculating the sum of the component dose rates:

$$\dot{D}_{tot} = (b\dot{D}_b + \dot{D}_{cap}), \qquad (2)$$

where $\dot{D}_b$ is the point-absorber infinite medium β dose rate, the constant b is a lumped correction factor related to attenuation effects and differences in electron stopping power between quartz and water, $\dot{D}_{cap}$ is the *in situ* γ and cosmic ray dose rate at the sampled location, measured using a dosemeter capsule, and corrected for the effects of attenuation of γ radiation in the dosemeter wall material. Where coarse quartz grains have been treated with strong acids to remove their outer layer, the α dose contribution can be neglected.

Experimental procedures

Sample preparation

The rear section of the sampled brick core was selected for analysis to reduce the contribution to the paleodose by radionuclides located beyond the immediate vicinity of the sampled core. The samples were prepared under dim red light conditions; from each brick core a slice of several mm thickness was cut at a depth of ~100mm from the outer surface of the brick using a water-lubricated diamond cutting wheel. The heterogeneity of the brick fabric was examined by visual inspection of the surface of the cut core. After removing the outer rim of the slice to a depth of ~2mm and cutting a segment for dose rate assessment, the remaining part of the slice was mechanically crushed and the material passed through sieves to isolate the grain size fractions 90–150μm and 150–200μm. Standard procedures for the quartz inclusion technique were applied to the sieved material to extract quartz grains. A portion of the 90–150μm (or 150–200μm) sieved fraction was immersed in hydrofluoric acid (HF; 40%) for a period of 45 minutes and, following a series of washing treatments, the etched material was immersed in hydrochloric acid (HCl) for 60 minutes to remove precipitates, after which it was washed and dried. The treated sample was sieved to remove grains < 90μm diameter (or 150μm for the 150–200μm fractions). The quality of the etched material was assessed by visual examination of one or more aliquots under a low power microscope in white light. The presence of feldspars in the etched material is routinely checked by examining for the presence of infra-red stimulated luminescence (IRSL) in aliquots - no significant IRSL emission was detected for the samples discussed in this report.

Paleodose

Luminescence measurements were performed using a Risø TL-DA-12 semi-automated reader and laboratory beta doses were administered using a calibrated $^{90}Sr/^{90}Y$ beta source (Göksu *et al* 1995) mounted in the reader. The luminescence was detected after passing through selected optical filters; for OSL and TL measurements, Hoya U340 filters (6mm) and no filter, respectively, were inserted. OSL decay curves were recorded using blue/green stimulation (450–550nm; ~30 mWcm^{-2}) and TL glow curves were recorded while heating the sample (5 ° s^{-1}) in an atmosphere of oxygen-free nitrogen.

Measurements were performed with sample aliquots of typically 1–2 mg of quartz. The grains were deposited as a near monolayer onto stainless steel discs that had previously been coated with a thin layer of silicone oil.

A sequence of initial tests (Table 4a) was performed to obtain the basic OSL and TL characteristics of each sample, including signal strength, response to absorbed dose, and degree of sensitisation. Examples of OSL decay curves and TL glow curves are shown in Figure 25a–c. On the basis of relatively poorer TL signal strength and the occurrence of sensitisation in some samples it was decided to determine the paleodose using OSL. However, preliminary estimates of the paleodose obtained by analysis of both the TL glow curves and OSL decay curves measured in these initial tests (for samples WSG-01–09) indicate nominal agreement within limits of experimental error (Fig 26a).

The paleodose was determined using an OSL single aliquot regeneration procedure (Bailiff and Holland 2000) based on the SAR technique (Wintle 1997), the main steps of which are given in Table 4b. In this procedure the background signal corresponds to the signal measured during the pre-heat monitor (steps 2, 4, 6, 8, 10, 12) and integrated between the start of the decay curve measurement and a time selected to provide optimum signal : background ratio (generally 800ms). The same integration interval was applied to all decay curves used to construct a dose response characteristic. An additive dose procedure was also applied to test for changes in luminescence properties during the first OSL measurement (Table 4b, Step 1, *β). Pre-heat temperatures, ranging from 200 to 280 °C, were applied to establish the existence of a plateau in the values of P. It is to be noted that more aggressive preheating was required with the Wimborne bricks compared with other brick samples tested in the laboratory. Additionally, diagnostic tests were performed with selected samples after the completion of paleodose measurements using an OSL scanner (Bailiff and Mikhailik 2003) to obtain maps of the distribution of OSL within aliquots.

Dose rate

The beta dose rate was determined using beta TL dosimetry (Bailiff 1982). Measurements were performed with pulverised brick in an unsealed state; the brick was taken from a portion of the same slice from which quartz was extracted for luminescence measurements. The activity of the brick was also measured using TSAC in both unsealed (α_0) and sealed condition (α_1) to obtain the combined uranium and thorium content and also to test for radon emanation during the first 24 h following sealing of the measurement chamber (Aitken 1985).

The combined gamma and cosmic dose rate at the sampled location was determined by means of gamma TL dosimetry. Dosimetry grade Al_2O_3:C (Akselrod *et al* 1990) in granular form (90–150μm) was annealed in the laboratory and packed into fused silica capsules (~3mm wall thickness, covered with an opaque plastic layer). These were placed into holes drilled adjacent to the coring location as discussed above (the period of measurement was 0.6 a). The accrued dose was determined using TL following a standard regeneration procedure where the laboratory beta dose was administered by the beta source mounted in the Risø reader, but where an aluminium absorber had been inserted below the irradiator aperture to provide a low dose rate (calibrated dose rate of 224 μGy min^{-1}), primarily due to bremmstrahlung.

Results

Ceramic fabric

The homogeneity of the brick fabrics was examined qualitatively by examining cut surfaces of cores using a binocular microscope and noting the presence of any large fragments of material that could add potentially differing radioactivity to the clay matrix (Table 5 and Figs 27a–b and 28a–l). Most of the samples appeared to have homogeneous fabrics, but WSG-01-2 and WSG-07-1 were noticeably heterogeneous with large coarse grains. Two examples of images obtained under low power magnification of slices cut from sample WSG-07-2 (Strong Room; WSG-07) are shown in Figure 27a–b.

Paleodose

Examples of a typical regenerative dose response characteristic showing good linearity and a plot of paleodose versus pre-heat temperature that exhibits a plateau are shown in Figures 29a and b respectively. The mean values of paleodose are given in Table 6. The results of the application of the additive dose procedure were used to construct a dose response characteristic similar to the modified additive dose procedure devised in the pre-dose technique (Haskell and Bailiff 1985) and also that employed in the SARA OSL procedure (Mejdahl and Bøtter-Jensen 1994) to detect changes in sensitivity. The estimate, P, was obtained by extrapolation of the characteristic to the dose axis. The values of P obtained using the two procedures, P_{ADD} and P_{SAR}, are in sufficient agreement (Fig 26b) to indicate the absence of a significant change in luminescence characteristics during the first OSL measurement.

Two samples (WSG-01-1 and WSG-02-1) were eliminated from further measurement due to inadequate OSL signal strength. The values of paleodose and dose rate obtained for samples WSG-07-1 and -2 and WSG-11 from the Strong Room were considered to yield unreliable dates and, hence, they are not included in Table 6. The main issue with these (early nineteenth-century) bricks is the possible heterogeneity in the beta radiation field due to the clustering of quartz grains (Fig 27b) and/or inhomogeneity in the brick fabric (Fig 27a), combined with significant differences in luminescence efficiency between grains (Fig 30a–d). Uncertainty associated with the dosimetry may arise if the luminescence measured with one aliquot were dominated by one grain (Fig 30a–b). In such cases where the fabric is complex the grain environment cannot be assumed to be typical of the bulk material that is used in TSAC and β-TLD measurements. Examples of two environments of a grain in a complex fabric are: i) when it is at the centre of a cluster of other quartz grains (lowest beta dose rate) or ii) it is a 'free' grain within a clay-rich fabric (highest beta dose rate). The beta dose rate is expected to differ significantly in these two environments. A more detailed examination of this issue was beyond the scope of this study.

Dose rate

The total dose rate for each sample and a breakdown of the percentage contribution due to beta and combined gamma and cosmic radiation dose rates are given in Table 6. The average proportions of beta ($\dot{D}_{\beta}$) and gamma plus cosmic ($\dot{D}_{\gamma+c}$) dose rates for all samples (expressed as a % of the total dose rate) are 54% and 46% respectively. Although the inner part of the sampled bricks were likely to have been nominally dry for a high proportion of the time since first use of the building, a nominal value of 5±5% moisture content was used in the calculation of the beta dose rate. Initially, the gamma dose rate was estimated on the basis of indirect measurement of ^{238}U, ^{232}Th and ^{40}K concentrations for the extracted core and the application of geometry factors related to the wall structure in the vicinity of each sample location (Bailiff 2001). The results later obtained from the *in situ* dosemeters provided a determination of the combined gamma and cosmic dose rate at each location, $\dot{D}_{cap}$, were used to calculate the values of $\dot{D}_{tot}$ inserted into the age equation. However, it is interesting to note that the combined dose rate obtained using the two approaches were found to be in good agreement (Fig 31).

The combined gamma and cosmic ray dose rate was also calculated for comparison with the value of $\dot{D}_{cap}$ using the following equation

$$\dot{D}_{tot} = (b\ \dot{D}_{\beta} + g\ \dot{D}_{\gamma} + \dot{D}_{cos}) \qquad (3)$$

where, in addition to the terms defined above, $\dot{D}_{\gamma}$ is the point-absorber infinite medium gamma ray dose rate, g is a lumped correction factor related to the geometry of the sources of gamma radiation and to differences in the absorption coefficient between ceramic and water, and $\dot{D}_{cos}$ is the annual dose due to cosmic rays (Prescott and Hutton 1988).

In deriving the total radiation beta dose rate from the results of beta-TLD measurements, it has been assumed that the distribution of naturally-occurring radionuclides within each slice (the volume from which the quartz was extracted) was homogeneous. However, there were doubts that this assumption was correct within the brick fabric for the bricks from the Strong Room (WSG-07 and WSG-11), as discussed above.

Luminescence dates

The values of the key parameters used to calculate the luminescence age are summarised in Table 6 for ten samples from a total of twelve locations. Ages were not calculated for samples from the Strong Room (WSG07-1, -2 and WSG-11; Locations WSG-07 and WSG-11) for reasons related to the heterogeneity in the composition of the brick fabric, as discussed above.

The average overall error (σ_B) corresponds to about ±7% of the luminescence age and this represents a reasonably good performance of the method.

As with all luminescence results, various assumptions have been made and factors taken into account, and they are summarised as follows:

i) The contribution to the paleodose due to alpha radiation was assumed to be negligible;

ii) The absence of a significant change in the values of sealed and unsealed alpha counts was taken to indicate that there was not a significant departure from secular equilibrium for the uranium and thorium chains;

iii) The gamma and cosmic dose rate measured with the Al_2O_3:C dosemeters was assumed to be representative of the average dose rate since construction of the relevant section of the building;

iv) The sampled walls were assumed not to have undergone substantial alteration following construction and it was assumed that recycled bricks had not been used;

v) The quartz grains used for luminescence measurements were assumed to have negligible uranium content.

Discussion

The suitability of bricks for luminescence dating depends on several factors including the luminescence properties of minerals, the composition of the brick fabric and firing conditions: these are expected to vary according to the age and origin of the bricks. Hence, this investigation reflects a mixture of the application of established measurement procedures and identification of factors that may require further study. In these circumstances the initial sampling plan had aimed to include locations for which there was secure dating evidence and where direct comparisons could be made between assigned architectural and luminescence dates. Although the dry-rot treatment that had been applied extensively throughout the brick fabric of the building limited the scope for sampling within the original plan, equivalent locations in safe sections of wall were identified and cored. Unfortunately, one of the locations with good chronological control (the Strong Room construction dated to AD 1810–15) contained bricks with problematic properties and OSL dates were not calculated.

Sampling by coring worked satisfactorily and the plugging of the core cavity with lime-based mortar and capping with the end slice of the brick core also appeared to be satisfactory (Fig 32), at least on initial inspection following completion of the reparation.

We chose to work with quartz crystals (about 1/10mm diameter) that were a constituent of the sand temper added during manufacture. As part of the initial evaluation phase of the laboratory work, the quartz extracts were tested using both OSL and TL techniques and, as discussed above, OSL was used for dating measurements because of its overall superior signal strength. However, in cases where the TL signal strength was adequate, the comparison of paleodose estimates indicated overall agreement within experimental limits.

Conclusion

The Wimborne study has demonstrated that the application of a routine luminescence technique to the dating of brick from a post-medieval building is feasible. Although the scope for sampling brick was limited by previous chemical treatments of the walls, it was possible to obtain brick cores from various key phases of construction with assigned architectural dates ranging from the seventeenth to nineteenth centuries. The majority of samples taken had suitable properties for luminescence dating, although the fabric of the early nineteenth-century bricks used at one location was found to be unsuitable due to fabric heterogeneity. The chronological model described below (Fig 37) has good overall agreement (A_{model}: 81) between the scientific dates and the architectural, structural, and documentary evidence. All the luminescence ages have good individual agreement with their places in this model (A > 60; Bronk Ramsey 1995, 429), except for WSG-02, which has poor individual agreement (A: 29). It appears to be rather late for its structural position as part of the east addition that was constructed in AD 1650–9. Detailed examination of the character of the brickwork (Fig 14c–e), however, clearly shows that this sample was taken from a brick that was part of the original construction of this range, and so this measurement is probably simply a slight statistical outlier.

Postscript 2017

This study, completed in 2003, represented an exploratory study of the luminescence testing of bricks from southern England and formed the basis of further methodological research with a wider temporal and geographical remit. This later research included the testing of buildings with tightly dated phases and enabled the consistency and accuracy of the method to be demonstrated in routine application (Bailiff 2007). Also, a series of studies of late medieval buildings in south eastern England (Gurling 2009) and north-west France (Blain 2009; Blain *et al* 2009) successfully demonstrated the general suitability of the method, accommodating different brick compositions and manufacturing techniques, and also confirmed the practice of using recycled brick by medieval masons (Bailiff *et al* 2010; Bailiff 2013).

RADIOCARBON DATING

Radiocarbon dating is based on the radioactive decay of ^{14}C and can be used to date organic materials, including wood. A small proportion of the carbon atoms in the atmosphere are of a radioactive form, ^{14}C. Living plants and animals take up carbon from the environment, and therefore contain a constant proportion of ^{14}C. Once a plant or animal dies, however, its ^{14}C decays at a known rate. This makes it possible to calculate the date of formerly living material from the concentration of ^{14}C atoms remaining. This ratio, which is reported with the uncertainty on the measurement, is known as a 'Radiocarbon age' and is reported in 'years' BP.

Radiocarbon ages are not the same as calendar dates because the concentration of ^{14}C in the atmosphere has fluctuated over time. This means that radiocarbon ages must be calibrated against an independent scale to arrive at the corresponding calendar date. That independent scale is the internationally agreed radiocarbon calibration curve, Intcal13 (Reimer *et al* 2013), which is based on tree-ring sequences which, once they have securely dated by dendrochronology, have in turn been radiocarbon-dated to define the differences between the radiocarbon and calendrical time-scales.

Figure 33 shows an example of a radiocarbon age that has been calibrated by the probability method (Stuiver and Reimer 1993), using the OxCal v.4.2 computer program (https://c14.arch.ox. ac.uk/oxcal/; Bronk Ramsey 1995; 2001; 2009) and IntCal13 (Reimer *et al* 2013). The resulting calibrated dates, expressed as 'cal AD', are typically multi-model probability distributions which span a century or more. This means that further statistical processing is required before the dates provided are sufficiently precise to be useful in research on historic buildings, such as St Giles House.

Further information about radiocarbon dating can be found in Bowman (1990).

Sampling

The small number of timbers that could be dated by dendrochronology in St Giles House, indeed the restricted number of timbers that were suitable for sampling for tree-ring analysis at all, left several major questions about the history of the building unresolved. In particular, calendar dating was needed for elements of the fabric that are clearly earlier than the building works undertaken in the AD 1650s.

Two timbers that had been cored for dendrochronology, but not dated by tree-ring analysis, were selected for radiocarbon dating in an attempt to provide information on this issue. Core wsgh04 was the third beam from the west in the hall ceiling, the putative former entrance in what is now the basement and core wsgh16b was one of the cores taken from the fireplace lintel in the Butler's Pantry/kitchen (Table 1a; Fig 6). Both were expected, on structural grounds, to pre-date the AD 1650s construction.

Timber wsgh04 contained 53 growth rings, possibly ending in the heartwood/sapwood transition. Six single-ring samples were taken from this core, spaced evenly through it with nine unsampled rings between each sample (and, thus, 10 years between the midpoint of one dated sample and the midpoint of the next in the series). Timber wsgh16b contained 31 growth rings ending in the heartwood/sapwood boundary. Six single-ring samples were taken from this core, space evenly through it with four unsampled rings between each sample (and, thus, five rings between the midpoint of one dated sample and the midpoint of the next in the series). Two rings were split across the growth-ring to ensure that each sample contained an equal proportion of wood laid down early in the growing season and wood laid down later in the year. These sub-samples were dated independently at two laboratories.

Laboratory methods

Seven samples were dated by the Oxford Radiocarbon Accelerator Unit (OxA-) in 2017. They underwent an acid-base-acid pretreatment followed by bleaching (Brock *et al* 2010, table 1 (UW)). They were then combusted and graphitized as described by Brock *et al* (2010, 110) and Dee and Bronk Ramsey (2000), and dated by Accelerator Mass Spectrometry (AMS) as described by Bronk Ramsey *et al* (2004). Seven samples were also dated by the Scottish Universities Environmental Research Centre (SUERC-) in 2017. They underwent chemical pretreatment to isolate α-cellulose, and were combusted, graphitised, and dated by AMS as described by Dunbar *et al* (2016).

Both laboratories maintain a continual programme of quality assurance procedures, in addition to participation in international inter-comparisons (Scott 2003; Scott *et al* 2007; 2010). These tests indicate no laboratory offsets and demonstrate the reproducibility and accuracy of these measurements. Three pairs of replicate measurements, obtained on the same ring, are all statistically consistent (Ward and Wilson 1978; Table 7) and have been combined by taking a weighted mean before calibration.

The results are conventional radiocarbon ages (Stuiver and Polach 1977; Table 7), and are quoted in accordance with the international standard known as the Trondheim convention (Stuiver and Kra 1986).

Calibration

The calibrations which relate the radiocarbon measurements directly to the calendrical time scale are shown in Figure 34. These have been calculated using IntCal13 (Reimer *et al* 2013), the probability method (Stuiver and Reimer 1993), and the computer program OxCal v4.2 (https://c14.arch.ox. ac.uk/oxcal/; Bronk Ramsey 1995; 2001; 2009). These are also the distributions shown in outline in the graphs illustrating the wiggle-matching reported below (Figs 35 and 36).

Wiggle-matching

Wiggle-matching uses information derived from tree-ring analysis in combination with radiocarbon dates to provide a revised understanding of the age of a timber; a review is presented by Galimberti *et al* (2004). In this technique, the shapes of multiple radiocarbon distributions can be 'matched' to the shape of the radiocarbon calibration curve. The exact interval of each radiocarbon date is known from tree-ring analysis, since one ring is laid down each year.

Although the technique can be done visually, Bayesian statistical analysis is now routinely employed. A general introduction to the Bayesian approach to interpreting archaeological data is provided by Buck *et al* (1996). The approach to wiggle-matching adopted here is described by Christen and Litton (1995).

Details of the algorithms employed in this analysis — a form of numerical integration undertaken using OxCal — are available from the on-line manual or from various publications by Christopher Bronk Ramsey (1995; 2001; 2009). Because it is possible to constrain a sequence of radiocarbon dates using the sequence and spacing of the samples provided by the tree-ring analysis, model outputs are posterior density estimates that are much more precise that simple calibrated radiocarbon dates. These posterior density estimates are shown in black in the Figures and quoted in italic in the text. They are rounded outwards to five years.

The A_{comb} statistic shows how closely the dates as a whole agree with other information in the model; an acceptable threshold is reached when it is equal to or greater than A_n, a value based on the number of dates in the model. The A statistic shows how closely an individual date agrees with the other information in the model; an acceptable threshold is reached when it is equal to or greater than 60.

The chronological model for core wsgh04, the ceiling beam in the hall, the putative former entrance, is shown in Figure 35. This includes the radiocarbon dates on the six single-year tree-ring samples (a weighted mean has been taken on the measurements from ring 12 before incorporation in the model) with the information that there were 10 calendar years between the mid-points of each in the sequence of dated samples. This model has good overall agreement (A_{comb}=149.5; (A_n=28.9); n=6), and all of the dates have good individual agreement as well. On the assumption that the heartwood/sapwood transition was present on this sample, the probability distribution of the likely number of sapwood rings missing from the timber (Miles 1997) has been added to the estimated date of the last surviving ring. This analysis suggests that this ceiling beam in the entrance hall (wsgh04) was felled in *cal AD 1540–1575* (*12% probability; wsgh04 felling*; Fig 35) or *cal AD 1645–1695 (83% probability)*, probably in *cal AD 1655–1680* (*68% probability*). If the heartwood/sapwood transition was not actually present on the timber, then this date estimate provides a *terminus post quem* for its felling.

The chronological model for core wsgh16b, the lintel over the fireplace in the kitchen, is shown in Figure 36. This includes the radiocarbon dates on the six single-year tree-ring samples (weighted means have been taken on the measurements from rings 7 and 25 before incorporation in the model) with the information that there were five calendar years between the mid-points of each in the sequence of dated samples. This model has good overall agreement (A_{comb}=129.7; (A_n=28.9); n=6), and all of the dates have good individual agreement as well. The probability distribution of the likely number of sapwood rings missing from the timber (Miles 1997) has been added to the estimated date of the last surviving ring, which in this case was clearly the heartwood/sapwood boundary. This analysis suggests that this timber (wsgh16) was felled in *cal AD 1485–1545* (*95% probability; wsgh04 felling*; Fig 36), probably in *cal AD 1495–1525* (*68% probability*). It is, thus, in all probability a reused timber reset in a part of the house dating from the mid-seventeenth century. If the timber came from an earlier house on the same site it would suggest a late fifteenth- or early sixteenth-century date for that.

BAYESIAN CHRONOLOGICAL MODELLING

This report has so far considered the results of the scientific dating undertaken on different elements of the fabric of St Giles House and the 'Riding House'. This analysis provides estimates for the dates when timbers were felled or bricks fired. Whilst this is of some interest in itself, what really matters is when those timbers or bricks were incorporated in the construction of various elements of these buildings. In the 'Riding House', only the timbers from the roof have been subject to scientific dating, and in this case dendrochronology clearly shows that this roof was constructed in AD 1616 or very shortly thereafter. St Giles House is a more complex story, and we need to combine various types of evidence – tree-ring dating, luminescence dating, radiocarbon wiggle-matching, structural and architectural analysis, and documentary records – into an integrated view of the history of the house.

Here, we do this formally, using Bayesian chronological modelling to combine explicitly the various strands of data. The principle behind the Bayesian approach to the interpretation of data is encapsulated by Bayes' theorem (Bayes 1763). It means that new data collected about a problem ('the standardised likelihoods') are analysed in the context of existing experience and knowledge of that problem ('prior beliefs'). The combination of the two permits a new understanding of the problem ('posterior beliefs') which can in turn become prior beliefs in a subsequent model. Bayesian analysis brings together architectural, structural, and documentary information with the scientific dates by expressing both as probability density functions, which are also the form of the posterior beliefs. This approach is particularly well suited to interpreting scientific dating information as this often takes the form of complex probability distributions.

In the modelling of St Giles House scientific dates form the 'standardised likelihoods' component of the model and architectural, structural, and documentary information provides the 'prior beliefs', so that the scientific dates are reinterpreted in the light of this independent information to provide posterior beliefs about the dates. Such estimates will vary with the model(s) employed, and several different models may be constructed based on varying interpretations of the same data (Bayliss *et al* 2007). The purpose of modelling is to progress beyond the scientific dates of individual samples to the dates of the episodes of construction that incorporated those samples in the building.

The chronological model for St Giles House is shown in Figure 37. It has been defined in OxCal v.4.2 (Bronk Ramsey 1995; 1998), detailing the scientific dates and specifying the known relative and calendar ages of the samples according to the architectural, structural, and documentary evidence (Fig 38).

Once the probability distributions of individual scientific dates have been calculated, the program attempts to reconcile these distributions with the prior information by repeatedly sampling each distribution to build up a set of solutions consistent with the model structure. This is done using a random sampling technique (Markov Chain Monte Carlo or MCMC), which generates a representative set of possible combinations of dates. This process produces a posterior probability distribution for each sample's calendar age, which occupies only a part of the calibrated probability distribution. In the case of wsgh04, for example, the estimate of the date of felling produced by the wiggle-matching *(cal AD 1540–1575 (12% probability; wsgh04 felling*; Fig 35) or *cal AD 1645–1695 (83% probability)*, probably *cal AD 1655–1680 (68% probability)*) is reduced to an estimate of *cal AD 1651–1659 (95% probability; wsgh04 felling*; Fig 37) or *cal AD 1655–1659 (68% probability)*.

Statistics calculated by OxCal provide guides to the reliability of a model. One is the individual index of agreement which expresses the consistency of the prior and posterior distributions. If the posterior distribution is situated in a high-probability region of the prior distribution, the index of agreement is high (sometimes 100 or more). If the index of agreement falls below 60 (a threshold value analogous to the 95% significance level in a χ^2 test) the scientific date is regarded as inconsistent with the sample's calendar age. Sometimes this merely indicates that the scientific date is a statistical outlier (more than two standard deviations from the sample's true radiocarbon age), but a very low index of agreement may mean that the sample was reused (ie that its calendar age is different to that implied by its stratigraphic position), or that the measurement is not accurate. Another index of agreement, A_{model}, is calculated from the individual agreement indices, and indicates whether the model as a whole is likely, given the data. This too has a threshold value of 60. The degree to which the MCMC has produced a truly representative set of solutions for the model is called convergence. A variety of diagnostic tools have been proposed to validate convergence, that employed by OxCal being described by Bronk Ramsey (1995, 429).

The model shown in Figure 37 has good convergence (C: 100) and good overall agreement (A_{model}: 81). The scientific dates are clearly compatible with the prior information included in the model that is illustrated in Figure 38. Only one luminescence date, WSG-02, has poor individual agreement in this model (A: 29). It appears to be rather late for its structural position as part of the east addition that was constructed in AD 1650–9. Detailed examination of the character of the brickwork (Fig 14c–e), however, clearly shows that this sample was taken from a brick that was part of the original construction of this range, and so this measurement is probably simply a slight statistical outlier.

DISCUSSION

The scientific dating programme reported here had two principal objectives: to determine whether luminescence dating could provide ages that were sufficiently accurate and precise that they can be used to aid the structural interpretation of a historic building, and to aid in the understanding of the surviving fabric of St Giles House and the 'Riding House' to inform a major repair programme. Both objectives have clearly been met (Fig 37).

Four of the samples taken for luminescence dating are from parts of the building whose date is clearly known from documentary evidence. WSG-02 and WSG-03 are from the east addition that was constructed in AD 1650–9, WSG-04 is from the small dining room that was part of works undertaken in AD 1670–4, and WSG09 is part of a block constructed by Flitcroft in AD 1740–5. With the exception of WSG-02, which is very slightly later than expected, all the luminescence ages are in good agreement with this dating. Two further known-age samples, WSG-07 and WSG-11 from the strong room constructed in AD 1810–15, could not be dated using luminescence.

Scientific dating has also clarified the extent of the documented construction phases. Luminescence dates from the basement (WSG-05 and WSG-12) show that the east addition of AD 1650–9 including re-building at this level, and that the mid sixteenth-century doorway has been reset. However, structural evidence such as an external brick plinth further south in the same wall suggests that some earlier walling was retained as part of the AD1650s buildings works. Another luminescence date (WSG-01) and the date for a wiggle-matched timber (*wsgh04*) show that this campaign extended a little further west than previously supposed, including both the north wall and the ceiling beams of the hall, the former putative entrance. Construction of the south range in AD 1670–4 was supplemented by works at the same time in the west range (suggesting that the works of AD 1670–4 were more comprehensive than previously thought), with works to both the upper brickwork in the Southampton Room being attested by luminescence dating (WSG-10) and re-roofing of the Handel room demonstrated by dendrochronology (Fig 10). Dendrochronology has also shown that the roof over the Southampton Room was replaced in AD 1735 or shortly thereafter (Fig 10).

Most elements of the surviving fabric that were thought to pre-date AD 1650 have been assigned by the scientific dating and structural phasing to later building campaigns. The original construction of the White Hall range, however, clearly predates this on structural grounds. Luminescence dating (WSG-06) in combination with the structural evidence suggests that this range was built in *AD 1633–1650 (95% probability; WSG06*; Fig 37), probably in *AD 1643–1650 (68% probability)*. It is *87% probable* that the brick dated from this work (*WSG06)* was fired after AD 1639, and so it appears plausible that this block was constructed by Sir Antony Ashley-Cooper when he gained possession of the estate following his coming of age in AD 1639. A timber dated by radiocarbon wiggle-matching from a lintel over the fireplace in the same area of walling, was felled in *cal AD 1480–1530 (94% probability; wsgh16b*; Fig 37) or *cal AD 1630–1640 (1% probability)*, probably in *cal AD 1490–1515 (68% probability)*, and is clearly reused in its present position. On historical grounds, the construction date for the White Hall range can perhaps be refined further.

CONCLUSION

A synthetic study has combined architectural, structural, and historical evidence with a series of dates on timbers produced by dendrochronology (Fig 10) and radiocarbon wiggle-matching (Figs 35 and 36) and bricks produced by luminescence dating (Table 6), using the explicit framework of Bayesian chronological modelling (Fig 37). This has refined the understanding of elements of the surviving fabric of both St Giles House and the 'Riding House', and demonstrates the potential of such multi-disciplinary studies to contribute to our understanding of historic buildings and their conservation and repair.

BIBLIOGRAPHY

Aitken, M J, 1985 *Thermoluminescence Dating*, London Academic Press

Aitken, M J, 1989 Luminescence dating: a guide for non-specialists, *Archaeometry*, **31**, 147–59

Aitken, M J, 1998 *An Introduction to Optical Dating: The Dating of Quaternary Sediments by the use of Photon-stimulated Luminescence, Oxford*, Oxford University Press

Akselrod, M S, Kortov, V S, Kravetsky, D J, and Gotlib, V I, 1990 Highly sensitive thermoluminescent anion defect in α- Al_2O_3:C single crystal detector, *Radiation Protection Dosimetry*, **32**,15–20

Arnold, A, and Howard, R, 2010 *St Firmin Church, Thurlby, Lincolnshire, Tree-ring analysis of timbers of the bellframe and tower*, English Heritage Res Dept Rep Ser, **72/2010**

Arnold, A, and Howard, R E, 2014 *Wood Barn, Fairfield House, Stogursey, Somerset, Tree-ring analysis of timbers*, English Heritage Res Rep Ser, **14/2014**

Bailiff, I K, 1982 Beta-TLD apparatus for small samples, *PACT*, **6**, 72–6

Bailiff, I K, 2001 Fallout dose evaluation: gamma dose rate geometry factors for brick walls, in *Dose reconstruction for populations in areas contaminated by Chernobyl fallout* (eds I K Bailiff and V Stepanenko), European Commission Contract IC15-CT96-0315 Final Report, Durham. University of Durham, Environmental Research Centre

Bailiff, I K, 2007 Methodological developments in the luminescence dating of brick from English late medieval and post medieval buildings, *Archaeometry*, **49**, 827–51

Bailiff, I K, Blain, S, Graves, C P, Gurling, T, and Semple, S, 2010 Uses and recycling of brick in medieval and Tudor English buildings: insights from the application of luminescence dating and new avenues for further research, *The Archaeological Journal*, **167**, 165–96

Bailiff, I K, 2013 Luminescence dating of brick from Brixworth church – re-testing by the Durham laboratory, in *The Anglo-Saxon Church at Brixworth, Northamptonshire: survey, excavation and analysis, 1972–2010* (D Parsons and D S Sutherland), Oxford, Oxbow Books, 243–250

Bailiff, I K, and Holland, N, 2000 Dating bricks of the last two millennia from Newcastle upon Tyne: a preliminary study, *Radiation Measurements*, **32**, 615–9

Bailiff, I K, and Mikhailik, V B, 2003 Spatially-resolved measurement of optically stimulated luminescence and time-resolved luminescence, *Radiation Measurements*, 37, 151–9

Baillie, M G L, and Pilcher, J R, 1973 A simple cross-dating program for tree-ring research, *Tree Ring Bulletin*, 33, 7–14

Bayes, T R, 1763 An essay towards solving a problem in the doctrine of chances, *Philosophical Transactions of the Royal Society*, 53, 370–418

Bayliss, A, Bronk Ramsey, C, van der Plicht, J, and Whittle, A, 2007 Bradshaw and Bayes: towards a timetable for the Neolithic, *Cambridge Archaeological Journal*, 17(1 suppl), 1–28

Berger, G W, Mulhern, P J, and Huntley, D H, 1980 Isolation of silt-sized quartz from sediments, *Ancient TL*, 11, 8–9

Blain, S, 2009 *Les terres cuites architecturales des églises du haut Moyen Age dans le nord-ouest de la France et le sud-est de l'Angleterre. Application de la datation par luminescence à l'archéologie du bâti. Ceramic building materials in early medieval churches in north-western France and south-eastern England. Application of Luminescence dating to building archaeology*, unpublished Dual Award PhD thesis, University of Bordeaux III and the University of Durham

Blain, S, Bailiff, I K, Guibert, P, Bouvier, A, and Baylé, M, 2009 An intercomparison study of luminescence dating protocols and techniques applied to medieval brick samples from Normandy (France), *Quaternary Geochronology*, 5, 311–6

Bowman, S, 1990 *Radiocarbon dating*, London British Museum

Bridge, M C, 1998 *Tree-ring analysis of timbers from the Chicheley Chapel, St Andrew's Church, Wimpole, Cambridgeshire*, Anc Mon Lab Rep, 59/98

Bridge, M C, 2003 unpubl Compilation of master chronologies from East Anglia, unpublished computer file ANGLIA03, University College London Dendrochronology Laboratory

Bridge, M C, 2014a *Church of St Andrew, Whitestaunton, Somerset, Tree-ring analysis of timbers from the bellframe and foundation beams*, English Heritage Res Rep Ser, 33/2014

Bridge, M C, 2014b *Sherborne House, Newland, Sherborne, Dorset, Tree-ring analysis of timbers from the Tudor Wing*, English Heritage Res Rep Ser, 31/2014

Bridge, M C, and Miles, D H, 2015 Tree-ring date lists: list 274 – Oxford Dendrochronology Project phase eleven, *Vernacular Architect*, 46, 108–12

Brock, F, Higham, T, Ditchfield, P, and Bronk Ramsey, C, 2010 Current pretreatment methods for AMS radiocarbon dating at the Oxford Radiocarbon Accelerator Unit (ORAU), *Radiocarbon*, 52, 103–12

Bronk Ramsey, C, 1995 Radiocarbon calibration and analysis of stratigraphy, *Radiocarbon,* 36, 425–30

Bronk Ramsey, C, 1998 Probability and dating, *Radiocarbon,* 40, 461–74

Bronk Ramsey, C, 2001 Development of the radiocarbon calibration program Oxcal, *Radiocarbon*, 43, 355–63

Bronk Ramsey, C, 2009 Bayesian analysis of radiocarbon dates, *Radiocarbon*, 51, 337–60

Bronk Ramsey, C, Higham, T, and Leach, P, 2004 Towards high-precision AMS: progress and limitations, *Radiocarbon*, 46, 17–24

Buck, C E, Cavanagh, W G, and Litton, C D, 1996 *Bayesian approach to interpreting archaeological data*. Chichester, John Wiley and Sons

Cattell, J, and Barson, S, 2003 *St Giles's House, Wimborne St Giles, Dorset*, English Heritage Historic Buildings and Areas Research Department Reports and Papers, B/023/2003

Christen, J, and Litton, C, 1995 A Bayesian approach to wiggle-matching, *Journal of Archaeological Science*, 22, 719–25

Dee, M, and Bronk Ramsey, C, 2000 Refinement of graphite target production at ORAU, *Nuclear Instruments and Methods Physics Research B*, 172, 449–53

Duller, G A T, 2008 *Luminescence Dating Guidelines on using luminescence dating in archaeology*, Swindon, English Heritage

Dunbar, E, Cook, G T, Naysmith, P, Tripney, B G, and Xu, S, 2016 AMS ^{14}C dating at the Scottish Universities Environmental Research Centre (SUERC) radiocarbon dating laboratory, *Radiocarbon*, 58, 9–23

English Heritage 1998 *Dendrochronology: guidelines on producing and interpreting dendrochronological dates*, London, English Heritage

Galimberti, M, Bronk Ramsey, C, and Manning, S W, 2004 Wiggle-match dating of tree-ring sequences, *Radiocarbon*, 46, 917–24

Göksu, H Y, Bailiff, I K, Bøtter Jensen, L, Hütt, G, 1995 Inter-laboratory beta source calibration using TL and OSL on natural quartz, *Radiation Measurements*, 24, 479–83

Groves, C, and Locatelli, C, 2004 *Tree-ring analysis of oak samples from Bushmead Priory, near Colmworth, Bedfordshire*, Centre for Archaeol Rep, 42/2004

Gurling, T, 2009 *Luminescence Dating of Medieval and Early Modern Brickwork*, unpublished PhD thesis, Durham University

Haddon-Reece, D, Miles, D H, Munby, J T, and Fletcher, J M, 1993 unpubl Oxfordshire Mean Curve - a compilation of master chronologies from Oxfordshire, OXON93, Oxford Dendrochronology Laboratory

Haskell, E H, and Bailiff, I K, 1985 Diagnostic and corrective procedures for predose TL analysis, *Nuclear Tracks*, 10, 503–8

Howard, R E, Laxton R R, and Litton, C D, 1998a *Tree-ring analysis of timbers from Chicksands Priory, Chicksands, Bedfordshire*, Anc Mon Lab Rep, 30/98

Howard, R E, Laxton R R, and Litton, C D, 1998b *Tree-ring analysis of timbers from 26 Westgate Street, Gloucester*, Anc Mon Lab Rep, 43/98

ISO 2004 International Vocabulary of Basic and General Terms in Metrology, 2nd ed. Revised *International Organisation for Standardization*, Geneva, Switzerland

Lane, R, 2016 *The Riding House, St Giles House, Wimborne St Giles, Building Investigation*, Historic England Res Rep Ser, 1/2016

Mejdahl, V, and Bøtter-Jensen, L, 1994 Luminescence dating of archaeological materials using a new technique based on single aliquot measurements, *Quaternary Geochronology*, 13, 551–4

Miles, D H, 1997 The interpretation, presentation, and use of tree-ring dates, *Vernacular Architect*, 28, 40–56

Miles, D W H, 2002 *Tree-Ring Dating of 8 Market Place, Shepton Mallet, Somerset*, Centre for Archaeol Rep, 4/2002

Miles, D, 2003 Dating Buildings and Dendrochronology in Hampshire, in *Hampshire Houses 1250 - 1700: Their Dating and Development* (ed E Roberts), 220–6, Southampton, Hampshire County Council

Miles, D H, 2004 unpubl Working compilation of reference chronologies centred around Somerset by various researchers, SOMRST04, Oxford Dendrochronology Laboratory

Miles, D, 2007 *Tree-Ring dating of the White Tower, HM Tower of London (TOL99 and TOL100), London Borough of Tower Hamlets*, English Heritage Res Dept Rep Ser, 35/2007

Miles, D H, and Bridge, M C, 2013 Tree Ring Dating Lists, *Vernacular Architecture*, 44, 98–102

Miles, D H, and Haddon-Reece, D, 1995 List 64 - Tree-ring dates, *Vernacular Architect*, **26**, 60–74

Miles, D H, and Worthington, M J, 1998 Tree-ring dates, *Vernacular Architect*, **29**, 111–29

Miles, D H, and Worthington, M J, 2000 Tree-ring dates, *Vernacular Architect*, **31**, 90–113

Miles, D H, Worthington, M J, and Bridge, M C, 2004 Tree-ring dates, *Vernacular Architect*, **35**, 95–113

Miles, D H, Worthington, M J, and Bridge, M C, 2005 Tree-ring dates, *Vernacular Architect*, **36**, 87–101

Miles, D H, Worthington, M J, and Bridge, M C, 2009 Tree-ring dates, *Vernacular Architect*, **40**, 122–31

Prescott, J R, and Hutton, J T, 1988 Cosmic-ray and gamma-ray dosimetry for TL and ESR. *Nuclear Tracks and Radiation Measurements*, **14**, 223–7

RCHME 1975 *An Inventory of Historical Monuments in the County of Dorset, Volume 5 East Dorset*, London, HMSO

Reimer, P J, Bard, E, Bayliss, A, Beck, J W, Blackwell, P G, Bronk Ramsey, C, Buck, C E, Cheng, H, Edwards R L, Friedrich, M, Grootes, P M, Guilderson, T P, Haflidason, H, Hajdas, I, Hatté, C, Heaton, T J, Hoffmann, D L, Hogg, A G, Hughen, K A, Kaiser, K F, Kromer, B, Manning, S W, Niu, M, Reimer, R W, Richards, D A, Scott, E M, Southon, J R, Staff, R A, Turney, C S M, and van der Plicht, J, 2013 Intcal 13 and marine13 radiocarbon age calibration curves 0–50,000 years cal BP, *Radiocarbon*, **55**, 1869–87

Scott, E M, 2003 The third international radiocarbon intercomparison (TIRI) and the fourth international radiocarbon intercomparison (FIRI) 1990–2002: results, analyses, and conclusions, *Radiocarbon*, **45**, 135–408

Scott, E M, Cook, G T, Naysmith, P, Bryant, C, and O'Donnell, D 2007 A report on phase 1 of the 5th international radiocarbon intercomparison (VIRI), *Radiocarbon*, **49**, 409–26

Scott, E M, Cook, G T, and Naysmith, P, 2010 A report on phase 2 of the fifth international radiocarbon intercomparison (VIRI), *Radiocarbon*, **52**, 846–58

Stuiver, M, and Kra, R S, 1986 Editorial comment, *Radiocarbon*, **28**(2B), ii

Stuiver, M, and Polach, H A, 1977 Reporting of ^{14}C data, *Radiocarbon*, **19**, 355–63

Stuiver, M, and Reimer, P J, 1993 Extended ^{14}C data base and revised CALIB 3.0 ^{14}C age calibration program, *Radiocarbon*, **35**, 215–30

Tyers, I, 1995 *Tree-ring analysis of Claydon House, Middle Claydon, Buckinghamshire*, Anc Mon Lab Rep, 13/95

Tyers, I, 2004 Dendro for Windows Program Guide 3rd edn, ARCUS Report, 500b

Ward, G K, and Wilson, S R, 1978 Procedures for comparing and combining radiocarbon age determinations: a critique, *Archaeometry*, 20, 19–31

Wilson, R, and Tyers, I, 1999 *Tree-ring analysis of oak timbers from the Church of St Mary the Virgin, Yatton, North Somerset*, Anc Mon Lab Rep, 61/1999

Wilson, R, Miles, D, Loader, N J, Melvin, T, Cunningham, L, Cooper, R, and Briffa, K, 2012 A millennial long March-July precipitation reconstruction for southern-central England, *Climate Dynamics*, 40, 997–1017

Wintle, A G, 1997 Luminescence dating: laboratory procedures and protocols, *Radiation Measurements*, 27, 769–817

Worthington, M, and Miles, D, 2006 *Tree-ring analysis of timbers from the Old Clarendon Building, Oxford, Oxfordshire*, English Heritage Res Dept Rep Ser, 67/2006

TABLES

Table 1a: Details of tree-ring samples taken from St Giles House, Wimborne St Giles, Dorset

Sample number	Timber and position	No of rings	Mean ring width (mm)	Dates spanning (AD)	h/s boundary date (AD)	Sapwood rings	Mean sensitivity	Felling date / date range (AD)
Basement Floor, south range								
wsgh01	South ceiling beam in Pantry (re-used)	64	2.80	-	-	h/s	0.22	-
wsgh02	North ceiling beam in Pantry (re-used)	49	2.97	-	-	h/s (+16NM)	0.18	-
Basement Floor, north range								
wsgh03	Second beam in Hall ceiling	<40	NM	-	-	-	-	-
wsgh04	Third beam in Hall ceiling	53	2.77	-	-	?h/s	0.19	-
Basement Floor, west range								
wsgh16a	Fireplace lintel in Butler's Pantry	38 (+1NM)	3.02	-	-	-	0.20	-
wsgh16b	ditto	31	2.59	-	-	h/s	0.18	-
Attic Floor, east range								
wsgh05	Floor beam in section A4	48	2.34	-	-	h/s	0.17	-
wsgh06	Floor beam between A4 and A5	<40	NM	-	-	-	-	-
Bedchamber Floor, Handel Room roof, west range								
wsgh07	West principal rafter, truss 2	60	2.11	-	-	12	0.22	-
wsgh08	Tiebeam, truss 2	63	2.48	-	-	-	0.16	-
wsgh09	East principal rafter, truss 2	95	1.88	1541–1635	1635	h/s	0.28	1644–76
wsgh10	West purlin, bay 2–3	72	1.38	1581–1652	1643	9 (+3NM)	0.15	1655–84
wsgh11	East principal rafter, truss 3	100	2.04	-	-	20 (+5NM)	0.18	-
wsgh12	East purlin, bay 3–4	81	1.70	1579–1659	1639	20	0.17	1659–80
wsgh13	East principal rafter, truss 4	54	2.72	1599–1652	1647	5	0.12	1656–88
Bedchamber Floor, Southampton Room, west range								
wsgh14	West upper strut, truss 1	64	1.87	1671–1734	1717	17C	0.26	winter 1734/35
wsgh15	West lower brace, truss 2	61	1.76	1656–1716	1716	h/s	0.17	1725–57

Key: NM = not measured; h/s = heartwood/sapwood boundary; C = complete sapwood, winter felled;

Table 1b: Details of the tree-ring samples from the 'Riding House', St Giles House, Wimborne, Dorset

Sample number	Timber and position	No of rings	Mean ring width (mm)	Dates spanning (AD)	h/s boundary date (AD)	Sapwood rings	Mean sensitivity	Felling date / date range (AD)
wsgr01	Tiebeam, truss 1	115	1.23	1501–1615	1596	19½C	0.13	summer 1616
wsgr02	South principal rafter, truss 1	88	2.25	1500–1587	1587	h/s (+19NM)	0.21	1606–28
wsgr03	South queen strut, truss 1	204	1.01	1411–1614	1593	21½C	0.21	summer 1615
wsgr04	North lower purlin, bay 1–2	51	2.56	-	-	17	0.25	-
wsgr05	North queen strut, truss 2	110	1.09	1492–1601	1600	1	0.18	1609–41
wsgr06	Tiebeam, truss 3	121	1.44	1476–1596	1596	h/s (+16NM)	0.15	1612–37
wsgr07	North principal rafter, truss 9	53	1.87	-	-	7 (+3NM)	0.31	-
wsgr08	Tiebeam, truss 5	118	1.23	1497–1614	1595	19½C	0.14	summer 1615
wsgr09	North principal rafter, truss 9	74	2.07	1532–1605	1588	17	0.16	1605–29
wsgr10	South lower purllin, bay 8–9	71	2.88	-	-	11 (+1NM)	0.20	-
wsgr11	Vertical post on stairs	<40	NM	-	-	-	-	-

Key: NM = not measured; h/s = heartwood/sapwood boundary; C = complete sapwood, winter felled; ½C = complete sapwood, felled the following summer

Table 2a: Cross-matching between the dated tree-ring series from the roof over the Handel Room (west range), St Giles House, Wimborne St Giles, Dorset; t*-values above 3.5 are statistically significant*

	t-values		
Sample	wsgh10	wsgh12	wsgh13
wsgh09	8.6	3.7	3.2
wsgh10		4.3	4.2
wsgh12			2.4

Table 2b: Cross-matching between the dated tree-ring series from the roof over the Southampton Room (west range), St Giles House, Wimborne St Giles, Dorset; t*-values above 3.5 are statistically significant*

	t-values
Sample	wsgh15
wsgh14	8.1

Table 2c:Cross-matching between the dated tree-ring series from the roof of the 'Riding House', St Giles House, Wimborne St Giles, Dorset; t*-values above 3.5 are statistically significant*

	t-values					
Sample	wsgr02	wsgr03	wsgr05	wsgr06	wsgr08	wsgr09
wsgr01	4.9	4.8	4.1	7.3	8.2	2.5
wsgr02		3.2	3.6	4.1	3.4	2,7
wsgr03			5.2	3.7	3.4	4.7
wsgr05				4.6	3.5	3.7
wsgr06					6.5	3.0
wsgr08						2.3

Table 3a: Dating evidence for the tree-ring site chronology WSGHHRR at AD 1541–1659

Source region	Chronology name	Publication reference	Filename	Span of chronology (AD)	Overlap (years)	*t*-value
Regional tree-ring reference chronologies						
South Central England	South Central England	Wilson *et al* 2012	SCENG	663–2009	119	5.5
Hampshire	Hampshire Master Chronology	Miles 2003	HANTS02	443–1972	119	5.4
Oxfordshire	Oxfordshire Master Chronology	Haddon-Reece *et al* 1993	OXON93	632–1987	119	5.2
Individual site tree-ring reference chronologies						
Somerset	8 Market Place, Shepton Mallet	Miles 2002	SHPTNMLT	1518–1677	119	6.8
Somerset	St Andrew's Church, Whitestaunton	Bridge 2014a	WHTSTNBF	1582–1676	78	6.5
Dorset	Sherborne House, Newland, Sherborne	Bridge 2014b	SHERHO1	1540–1670	119	6.0
Oxfordshire	Old Clarendon Building, Oxford	Worthington and Miles 2006	CLRNDNOX	1539–1711	119	5.9
Somerset	Church of St Mary the Virgin, Yatton	Wilson and Tyers 1999	YATTON 2	1564–1691	96	5.8
Hampshire	The Vyne, Sherbourne St John	Miles and Worthington 1998	THEVYNE3	1543–1653	111	5.7
Oxfordshire	Manor Farm, Stanton St John	Miles and Worthington 1998	STNSTJN4	1480–1646	106	5.7
Wiltshire	Salisbury Cathedral	Miles *et al* 2005	SARUM13	1557–1719	83	5.7
Wiltshire	Bishop's Palace, Salisbury	Miles and Worthington 2000	SARUMBP7	1562–1661	98	5.4

Table 3b: Dating evidence for the tree-ring site chronology sequence WSGH1415 at AD 1656–1734

Source region	Chronology name	Publication reference	Filename	Span of chronology (AD)	Overlap (years)	*t*-value
Regional tree-ring reference chronologies						
East Anglia	East Anglia Master Chronology	Bridge 2003	ANGLIA03	944–1789	79	6.1
South Central England	South Central England	Wilson *et al* 2012	SCENG	663–2009	79	6.0
Hampshire	Hampshire Master Chronology	Miles 2003	HANTS02	443–1972	79	5.2
Individual site tree-ring reference chronologies						
Wiltshire	Bishop's Palace, Salisbury	Miles and Worthington 2000	SARUMBP8	1616–1735	79	7.5
Somerset	Fairfield House barn, Stogursey	Arnold and Howard 2014	FRFBSQ01	1561–1771	79	6.9
Wiltshire	Salisbury Cathedral	Miles *et al* 2005	SARUM13	1557–1719	64	6.6
Buckinghamshire	Claydon House, Middle Claydon	Tyers 1995	CLAYDON	1613–1756	79	6.4
Bedfordshire	Chicksands Priory, Chicksands	Howard *et al* 1998a	CHKSPQ02	1611–1814	79	5.9
Bedfordshire	Bushmead Priory, Colmworth	Groves and Locatelli 2004	BUSHMEAD	1599–1709	54	5.7
London	White Tower, Tower of London	Miles 2007	WHTOWR8	1645–1732	77	5.6
Cambridgeshire	St Andrew's Church, Wimpole	Bridge 1998	WIMPOLE2	1667–1729	63	5.6
Lincolnshire	St Firmin's Church, Thurlby	Arnold and Howard 2010	THUBSQ01	1599–1792	79	5.6

Table 3c: Dating evidence for the site tree-ring chronology WSGRIDHO at AD 1411–1615

Source region:	Chronology name:	Publication reference:	File name:	Span of chronology (AD)	Overlap (years)	*t*-value
Regional tree-ring reference chronologies						
Hampshire	Hampshire Master Chronology	(Miles 2003)	HANTS02	443–1972	205	10.2
South Central England	South Central England	(Wilson *et al* 2012)	SCENG	663–2009	205	9.5
Somerset	Somerset Master Chronology	(Miles 2004)	SOMRST04	770–1979	205	9.1
Individual tree-ring site reference chronologies						
Gloucestershire	26 Westgate Street, Gloucester	(Howard *et al* 1998b)	GLOUC_WS	1399–1622	205	8.6
London	Henry VIII alterations, Hampton Court	(Miles and Bridge 2013)	HMPTNCT6	1351–1533	123	8.5
London	White Tower, Tower of London	(Miles 2007)	WHTOWR6	1370–1532	122	8.0
Wiltshire	Dog Kennel Farm, Clarendon	(Miles *et al* 2004)	CLRENDN7	1351–1603	193	7.9
Oxfordshire	Greys Court, Rotherfield Greys	(Miles *et al* 2009)	GREYSCTA	1319–1618	205	7.8
Hampshire	Abbots Barton farmhouse, Winchester	(Miles and Worthington 1998)	ABTSBRTN	1387–1559	149	7.8
Oxfordshire	Six Bells, Warborough	(Bridge and Miles 2015)	SIXBELLS	1364–1463	53	7.7
Worcestershire	Mere Hall, Hanbury	(Miles *et al* 2005)	MEREHALL	1408–1610	200	7.6
Hampshire	Exton Farm barn, Exton	(Miles and Haddon-Reece 1995)	EXTON	1376–1546	136	7.5

Table 4a: Summary of initial tests, single aliquot regeneration (OSL = 100 s stimulation, sample held at 125 °C during stimulation; PH = Pre-heat: RT selected temp, heat @ 5 °/s and hold for 10 or 20 s; β= estimated palaeodose (P); Aliq = aliquot).

Step	Procedure	Comments
1	PH; OSL	PH temp = 200 °C (Aliq #1); 220 °C (Aliq #2); 240 °C (Aliq #3) etc
2	PH; OSL	Pre-heat monitor
3	+ β; PH; OSL	B dose followed by preheat and measurement of OSL decay curve
4	PH; OSL	Pre-heat monitor
5	+0.5 β; PH; OSL	
6	PH; OSL	Pre-heat monitor
7	+2 β; PH; OSL	
8	PH; OSL	Pre-heat monitor
9	+3 β; PH; OSL	
10	PH; OSL	Pre-heat monitor
11	+ β; PH; OSL	Sensitization monitor
12	PH; OSL	Pre-heat monitor

*Table 4b: Generalised procedure for determination of palaeodose, single aliquot regeneration (OSL = 100 s stimulation, sample held at 125 °C during stimulation; PH = Preheat: RT selected temp, heat @ 5 °/s and hold at temperature for selected period (eg 10 s); β= estimated palaeodose (P); Aliq = aliquot; (*β) = administration of a β dose, β, in the additive dose procedure, and the values of the beta does in subsequent irradiations are increased by the value of β*

Step	Procedure	Comments
1	(*β); PH; OSL	PH temp = 200 °C (Aliq #1); 220 °C (Aliq #2); 240 °C (Aliq #3); 260 °C (Aliq #4; 280 °C (Aliq #5)
2	PH; OSL	Pre-heat monitor
3	+ β; PH OSL	Beta dose followed by preheat and measurement of decay curve
4	PH; OSL	Pre-heat monitor
5	+0.8 β; PH; OSL	
6	PH; OSL	Pre-heat monitor
7	+1.2 β; PH; OSL	
8	PH; OSL	Pre-heat monitor
9	+ β; PH; OSL	Sensitization monitor
10	PH; OSL	Pre-heat monitor

Table 5: Summary of macroscopic brick fabric characteristics, images of which are shown in Figure 28

Sample	Comments on fabric
WSG-01-1	Slight inhomogeneity; minor fragments
WSG-01-2	Highly inhomogenous; many fragments
WSG-02-1	Relatively homogeneous
WSG-02-2	Slight inhomogeneity; minor fragments
WSG-03	Relatively homogeneous
WSG-04	Slight inhomogeneity; minor fragments
WSG-05	Slight inhomogeneity; minor fragments
WSG-06	Relatively homogeneous
WSG-07-1	Inhomogeneous; many fragments
WSG-07-2	Inhomogeneous; many fragments
WSG-08	Relatively homogeneous
WSG-09	Relatively homogeneous

Table 6: Summary of palaeodose and dose rate values and luminescence ages

Sample	Palaeodose P (mGy)	Dose rate $\dot{D}_{tot}$ (mGy/a)	Dose rate components		Moisture % brick	Luminescence Date (AD)	Date Reference
			β (%)	γ+$_{cos}$ (%)			
WSG-01-2	815±21	2.49±0.09	57	43	5±5	1676 ±14; ±22	Dur03OSLqi-295-1-2
WSG-02-2	693±8	2.22±0.08	52	48	5±5	1691 ±12; ±20	Dur03OSLqi-295-2-2
WSG-03	667±18	1.89±0.07	48	52	5±5	1650 ±16; ±24	Dur03OSLqi-295-3
WSG-04	694±18	2.23±0.08	52	48	5±5	1692 ±14; ±21	Dur03OSLqi-295-4
WSG-05	778±9	2.33±0.08	51	49	5±5	1669 ±12 ±21	Dur03OSLqi-295-5
WSG-06	825±17	2.41±0.09	55	45	5±5	1660 ±14; ±23	Dur03OSLqi-295-6
WSG-07-1	-	3.01±0.13	58	42	5±5	-	
WSG-07-2	-	3.55±0.15	64	36	5±5	-	
WSG-08	908±7	2.52±0.09	56	44	5±5	1643 ±13; ±23	Dur03OSLqi-295-8
WSG-09	809±29	2.96±0.11	63	37	5±5	1730 ±14; ±20	Dur03OSLqi-295-9
WSG-10	846±10	2.57±0.09	58	42	5±5	1675 ±12; ±21	Dur03OSLqi-295-10
WSG-11	-	3.27±0.12	67	33	5±5	-	
WSG-12	747±18	2.23±0.08	55	45	5±5	1670 ±14; ±22	Dur03OSLqi-295-12

Table 7: Radiocarbon and stable isotopic results from St Giles House, Wimborne St Giles; replicate measurements have been tested for compatibility and combined before calibration as described by Ward and Wilson (1978)

Laboratory number	Sample identifier	Material	$\delta^{13}C$ (‰)	Radiocarbon age (BP)	Weighted mean (BP)
West Range kitchen: core wsgh16b					
SUERC-73414	ring 2	Wood, *Quercus* sp. heartwood	−23.8±0.2	357±32	
SUERC-73418	ring 7.A	Wood, *Quercus* sp. heartwood	−24.0±0.2	397±32	386±21 BP; T′=0.2, T′(5%)= 3.8, ν=1
OxA-35709	ring 7.B	Wood, *Quercus* sp. heartwood	−24.9±0.2	378±26	
OxA-35710	ring 13	Wood, *Quercus* sp. heartwood	−24.5±0.2	405±26	
SUERC-73419	ring 19	Wood, *Quercus* sp. heartwood	−25.1±0.2	373±32	
OxA-35711	ring 25	Wood, *Quercus* sp. heartwood	−25.6±0.2	347±28	362±20 BP; T′=0.5, T′(5%)= 3.8, ν=1
OxA-35712	ring 25	Wood, *Quercus* sp. heartwood	−25.8±0.2	375±27	
SUERC-73420	ring 30	Wood, *Quercus* sp. heartwood	−24.9±0.2	374±32	
North Range: core wsgh04					
OxA-35705	ring 2	Wood, *Quercus* sp. heartwood	−25.3±0.2	365±26	
OxA-35706	ring 12.A	Wood, *Quercus* sp. heartwood	−25.4±0.2	374±26	381±21 BP; T′=0.2, T′(5%)= 3.8, ν=1
SUERC-73411	ring 12.B	Wood, *Quercus* sp. heartwood	−24.1±0.2	392±32	
SUERC-73412	ring 22	Wood, *Quercus* sp. heartwood	−26.2±0.2	349±32	
OxA-35707	ring 32	Wood, *Quercus* sp. heartwood	−25.5±0.2	348±26	
SUERC-73413	ring 42	Wood, *Quercus* sp. heartwood	−26.0±0.2	274±32	
OxA-35708	ring 52	Wood, *Quercus* sp. heartwood	−26.0±0.2	260±26	

FIGURES

Figure 1: St Giles House view from the SE (© Historic England, DP167051; photograph by James Davies)

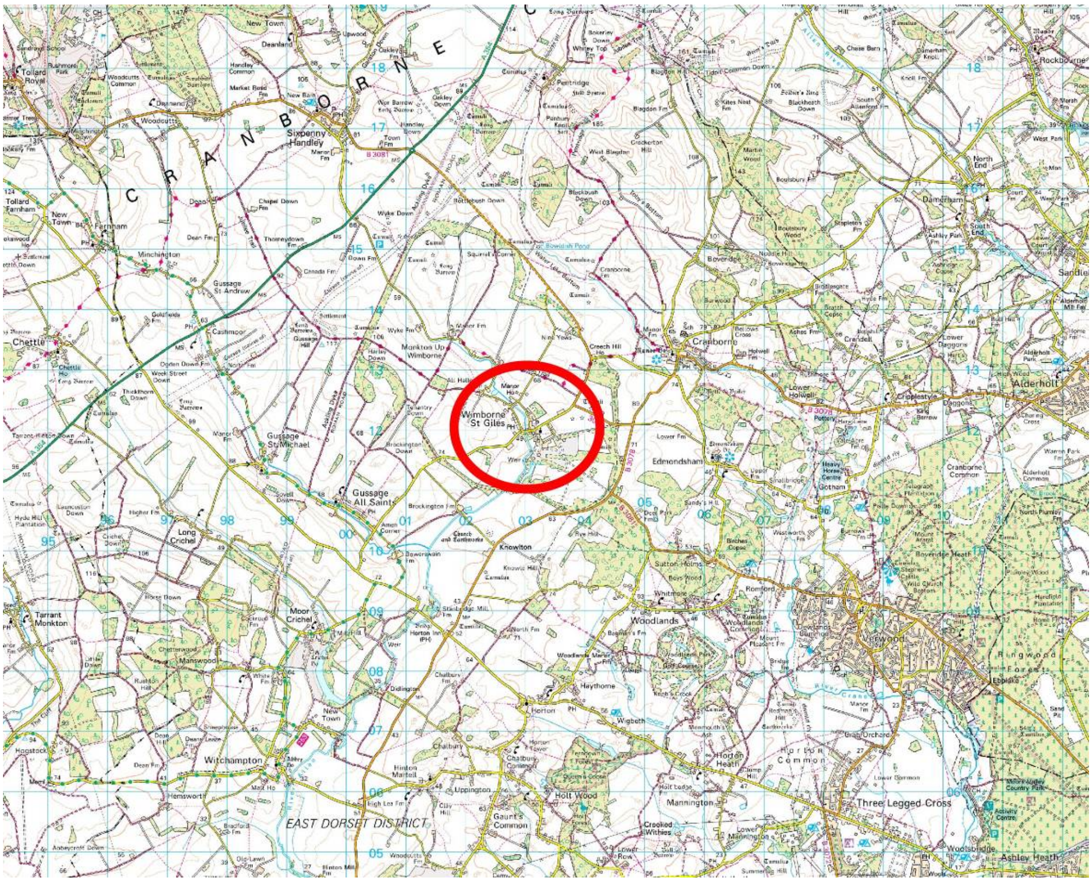

Figure 2: General location of Wimborne St Giles with the area of the House and 'Riding House' outlined in red. © Crown Copyright and database right 2018. All rights reserved. Ordnance Survey Licence number 100024900

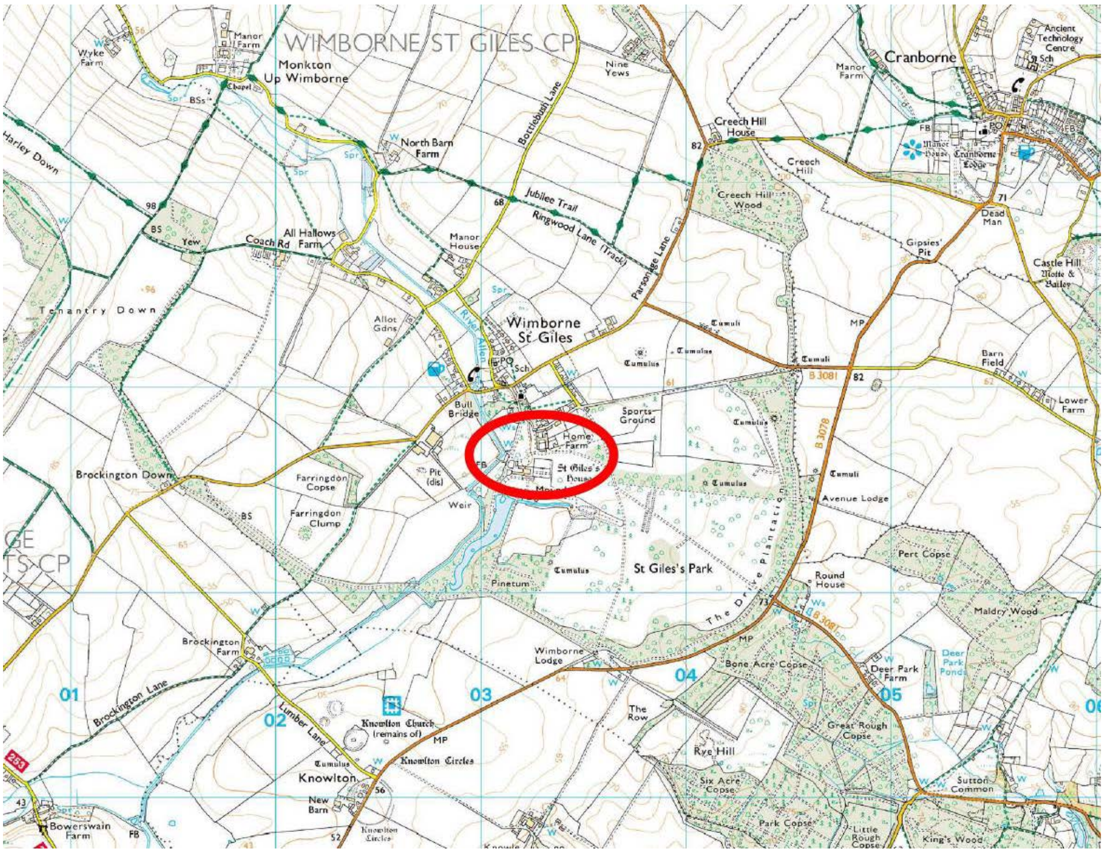

Figure 3: Location of St Giles House and 'Riding House' within Wimborne St Giles. © Crown Copyright and database right 2018. All rights reserved. Ordnance Survey Licence number 100024900

Figure 4: The relative locations of the St Giles House and the 'Riding House' within the estate. © Crown Copyright and database right 2018. All rights reserved. Ordnance Survey Licence number 100024900

Figure 5: The 'Riding House' (© Historic England, DP166132; photograph by James Davies)

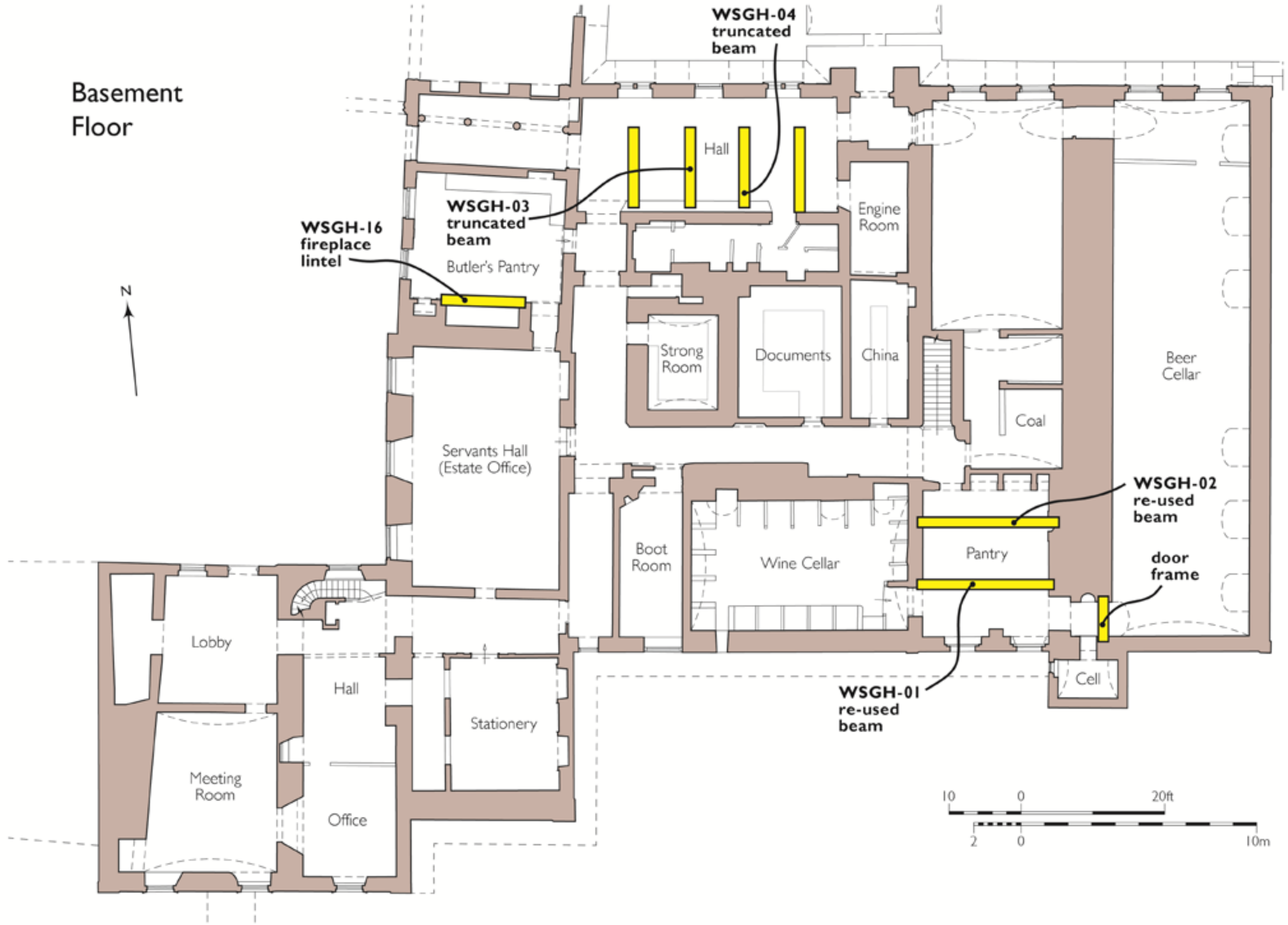

Figure 6: Plan showing the locations of timbers sampled for dendrochronology and radiocarbon dating at basement level in St Giles House, Wimborne St Giles (after Phillip Hughes Associates 2017)

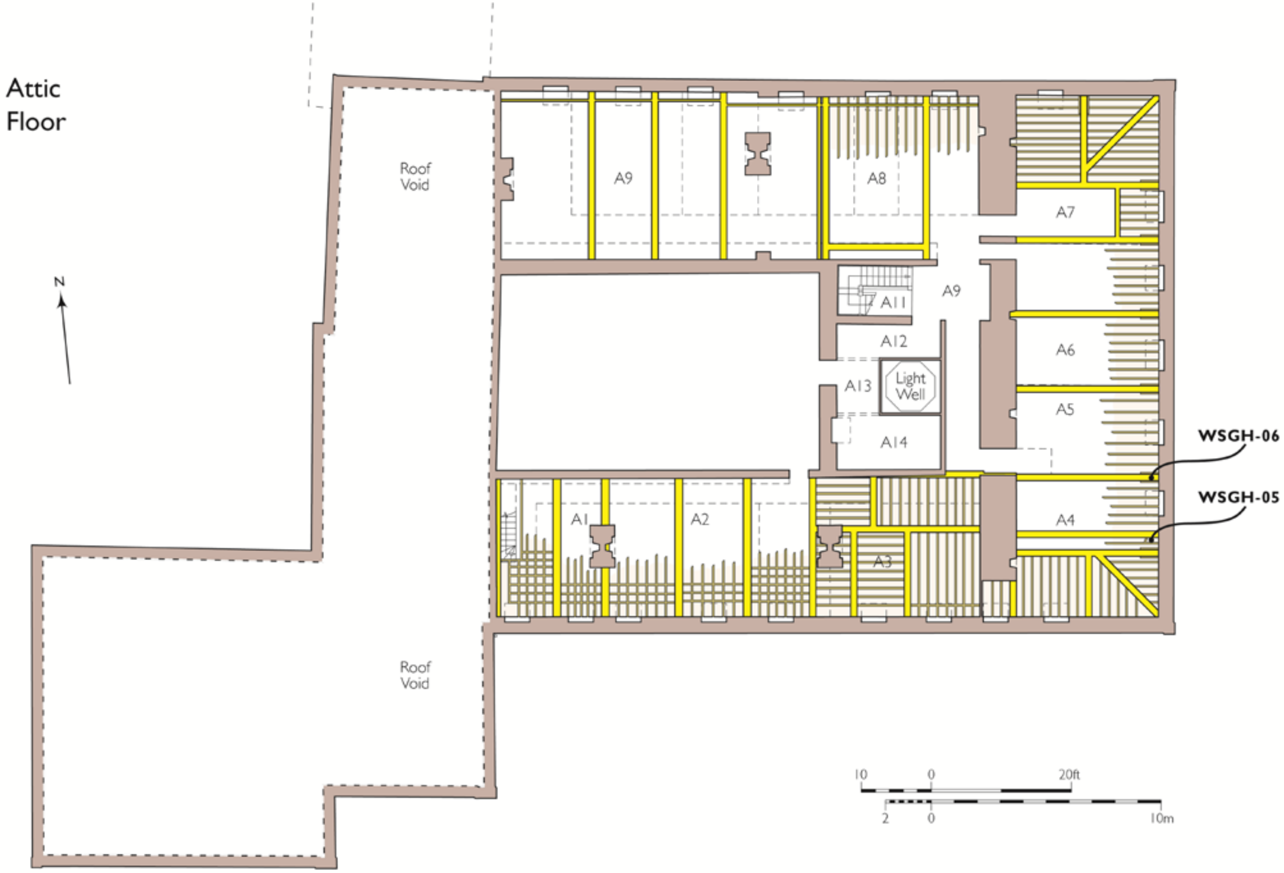

Figure 7: Plan of the eastern attics of St Giles House, showing the location of two timbers sampled for dendrochronology (after Phillip Hughes Associates 2017)

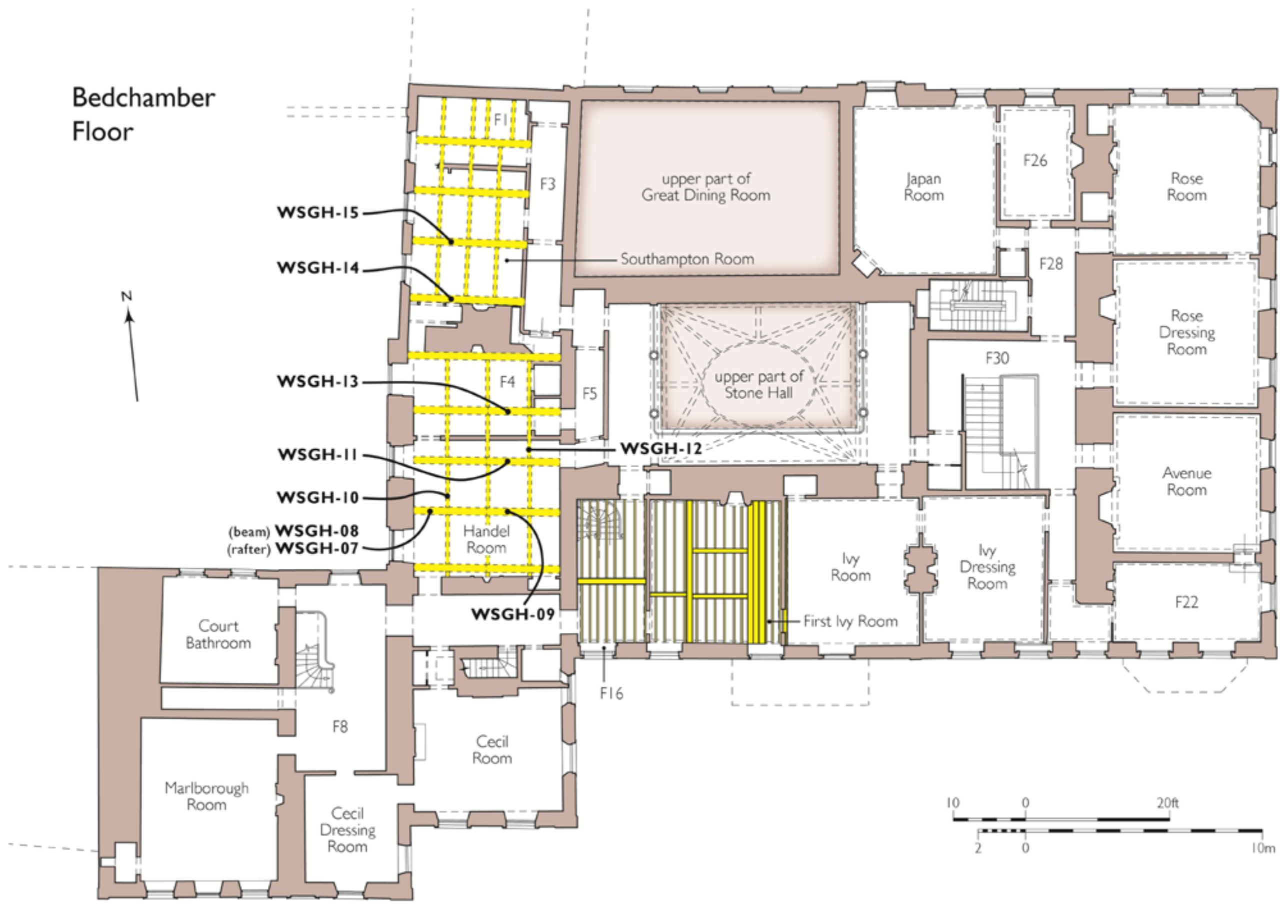

Figure 8: Plan of the south-west corner of St Giles House, showing the location of the Handel Room, over which the roof was sampled for dendrochronology (after Phillip Hughes Associates 2017)

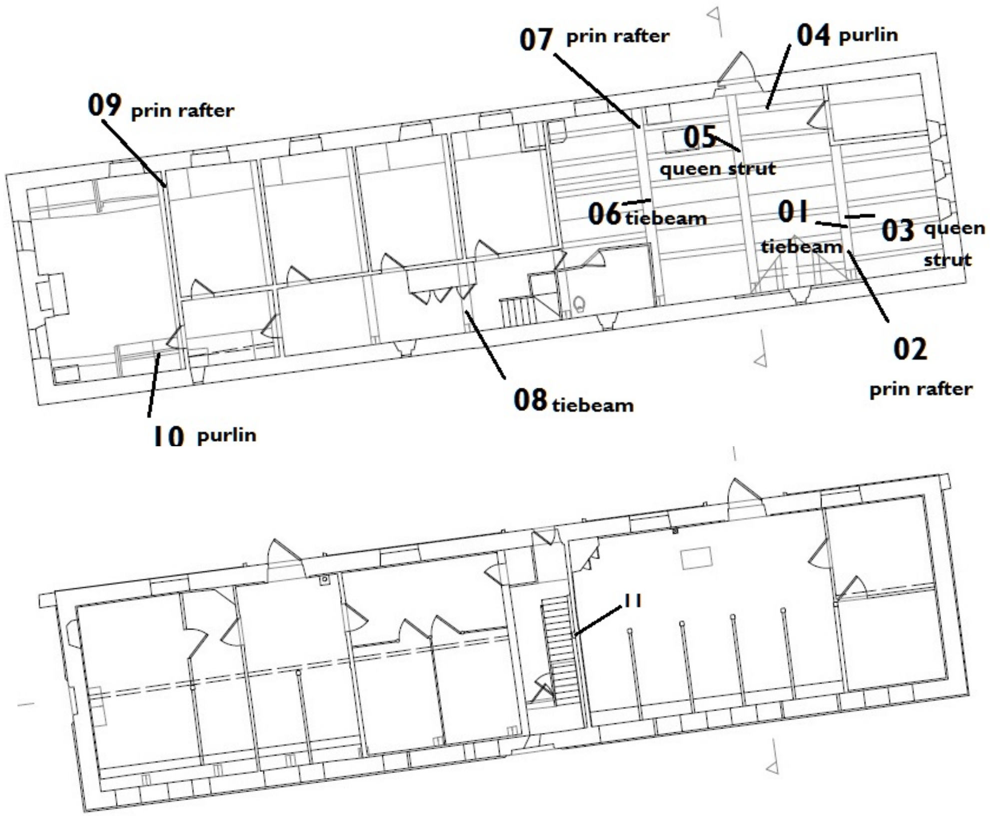

Figure 9: Plan of the 'Riding House' showing the locations of the timbers sampled (after Phillip Hughes Associates 2017)

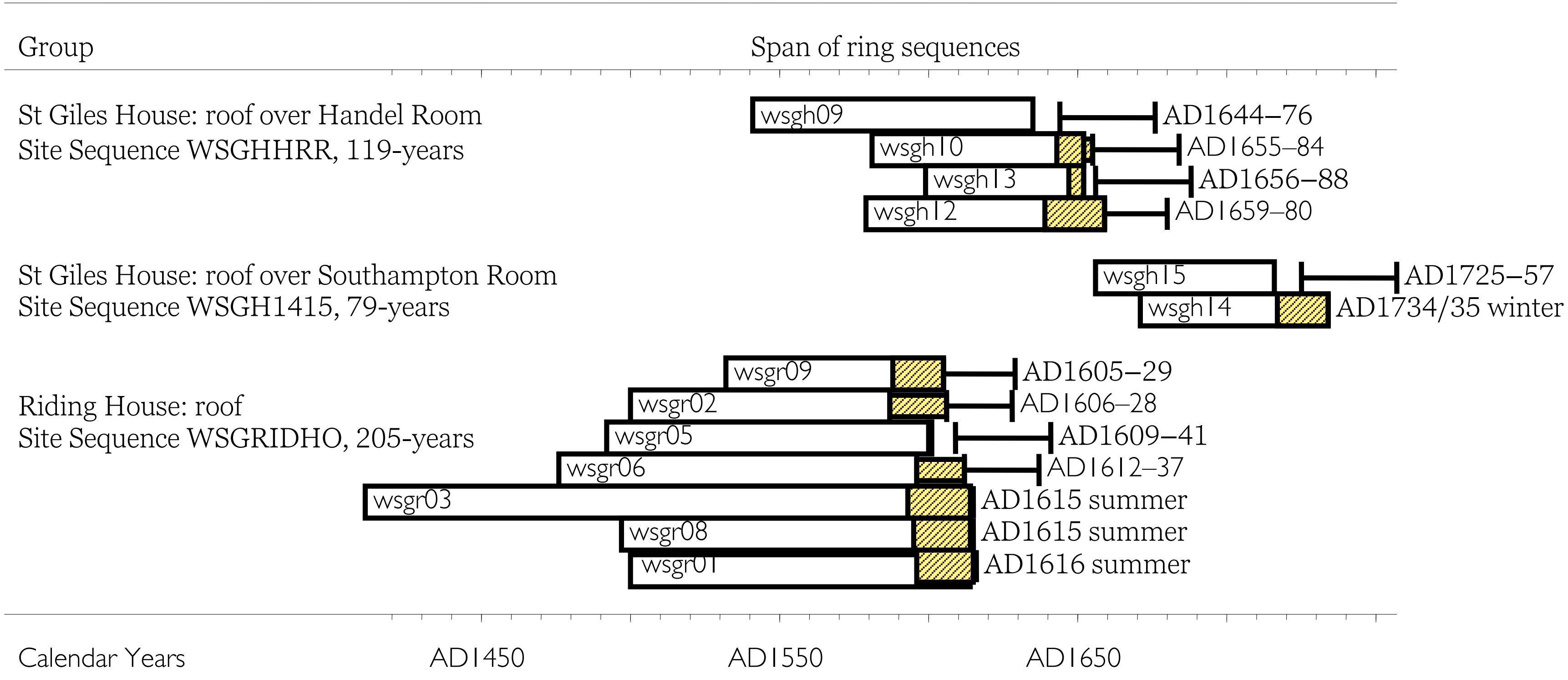

Figure 10: Bar diagram showing the relative positions of overlap and actual or likely felling date ranges for the dated samples from the 'Riding House', and St Giles House, Wimborne St Giles, Dorset. White bar – heartwood; yellow hatched bar – sapwood; narrow section bars – additional unmeasured rings

Figure 11: Plan of the basement/cellars of St Giles House, showing the location of bricks sampled for luminescence dating (after Phillip Hughes Associates 2017)

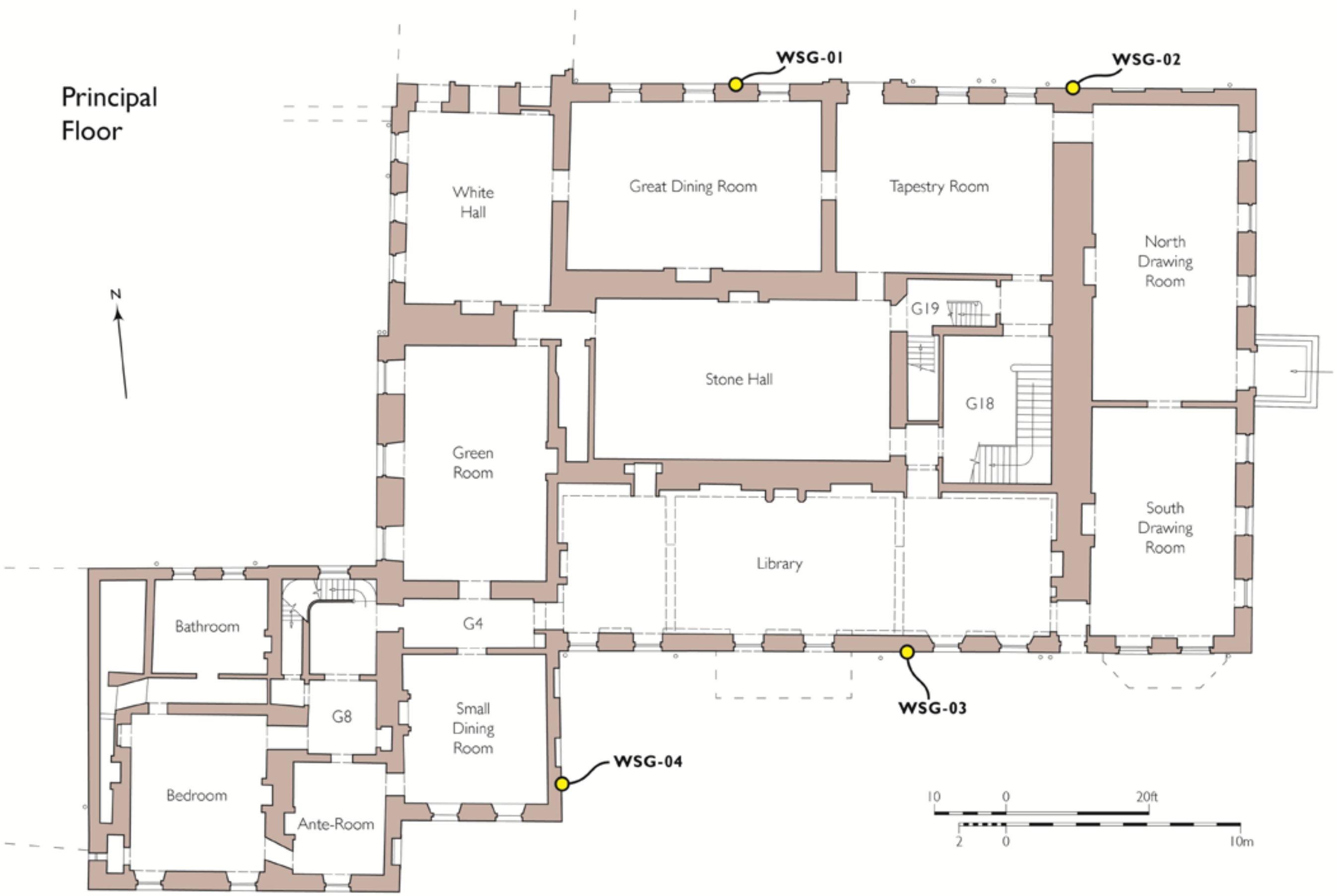

Figure 12: Plan of the principal floor of St Giles House, showing the location of bricks sampled for luminescence dating (after Phillip Hughes Associates 2017)

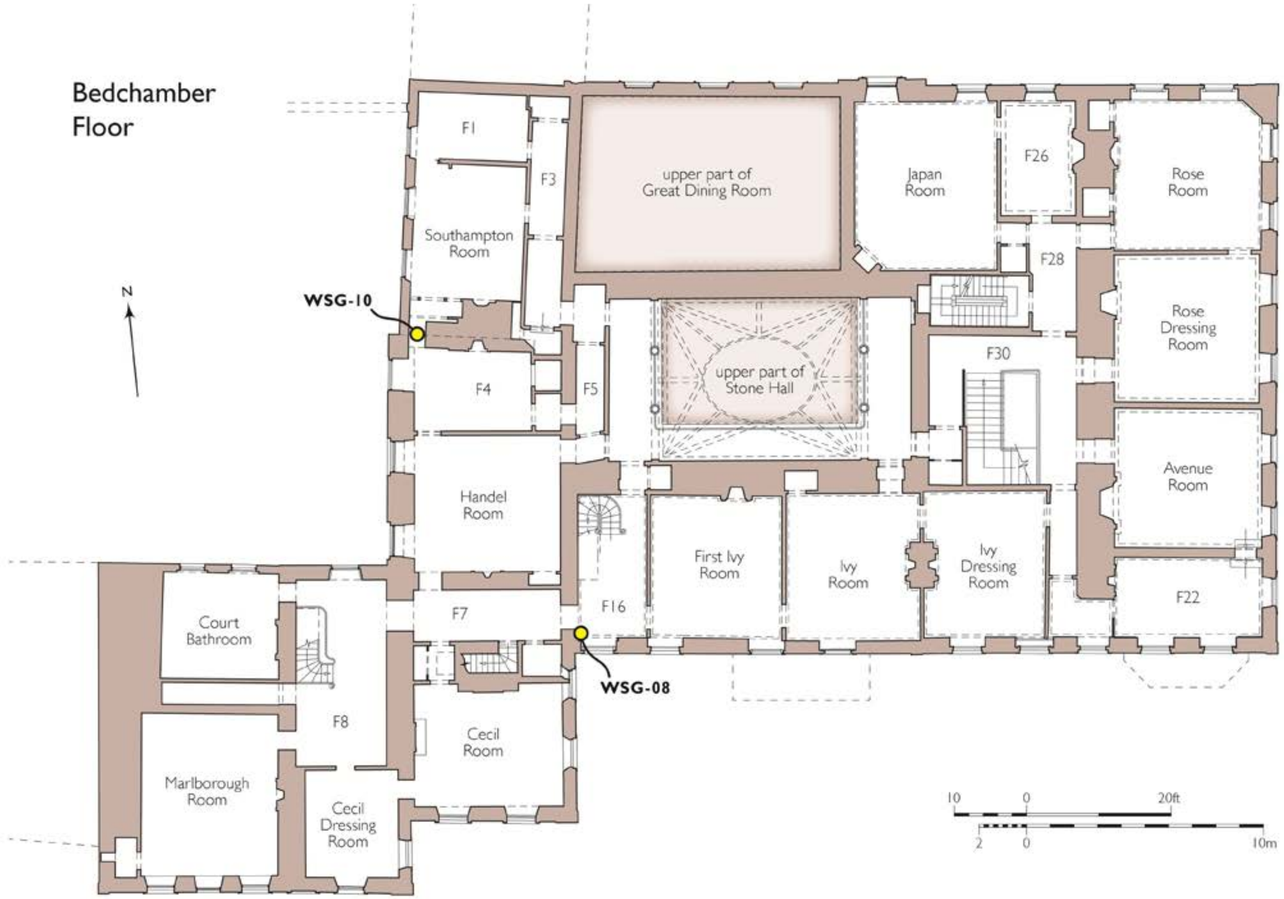

Figure 13: Plan of the bedchamber floor of St Giles House, showing the location of bricks sampled for luminescence dating (after Phillip Hughes Associates 2017)

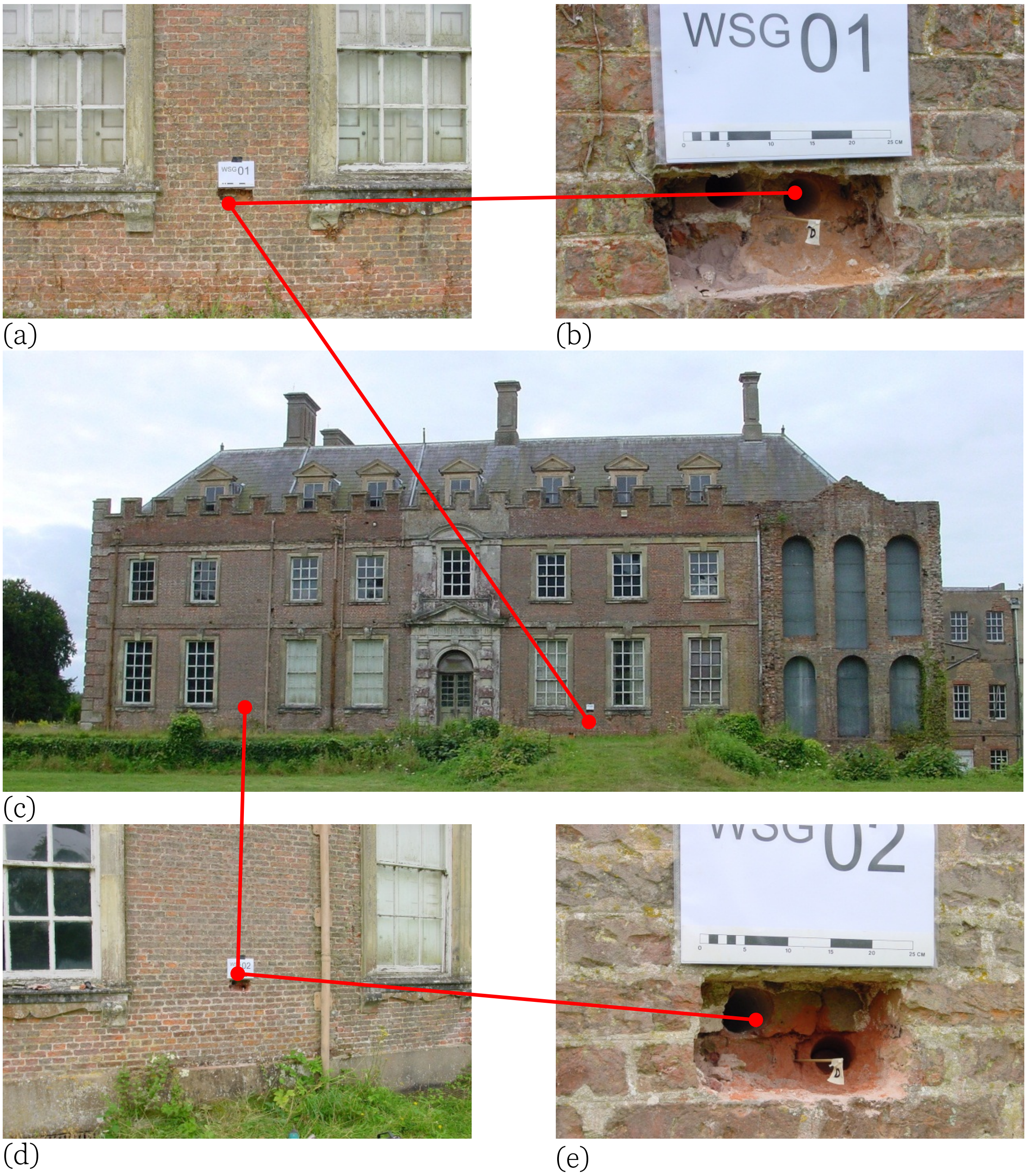

Figure 14: (a) section of north-facing wall showing location of WSG-01, (b) close-up of sampling location WSG-01, showing the position of cores WSG-01-1 (left), WSG-01-2 (right), and the dosemeter (flag D), (c) north-facing wall of St Giles House showing white card to right of entrance that indicates the location of WSG-01 and white card to left of entrance that indicates the location of WSG-02, (d) section of north-facing wall showing location of WSG-02, and (e) close-up of sampling location WSG-02 showing cores WSG-02-1 (upper left) and WSG-02-2 (lower right)

(a) (b)

Figure 15: (a) section of south-facing wall showing location of WSG-3, (b) close-up of sampling location WSG-3

(a) (b)

Figure 16: (a) section of east-facing wall of rear of house (small dining room) showing location of WSG-04, (b) close-up of sampling location WSG-04

Figure 17: section of west-facing interior wall of engine room showing sampling location WSG-05

(a) (b)

Figure 18: (a) section of north-facing interior wall of the west range adjacent to the kitchen fireplace in the basement showing location of WSG-06, (b) close-up of sampling location WSG-06 showing core hole and dosemeter (flag D)

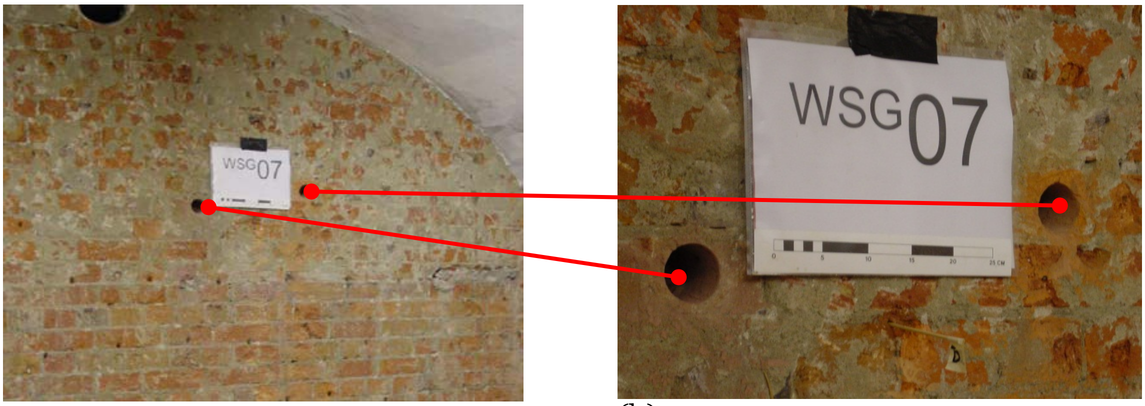

(a) (b)

Figure 19: (a) section of south-facing interior wall of strong room adjacent to fireplace showing locations WSG-07-1 and WSG-07-2, (b) close-up of sampling locations of cores WSG-07-1 (left), WSG-07-2 (right), and dosemeter (flag D)

Figure 20: section of interior wall on upper floor adjacent to south-facing window showing locations WSG-08 and dosemeter below (flag D)

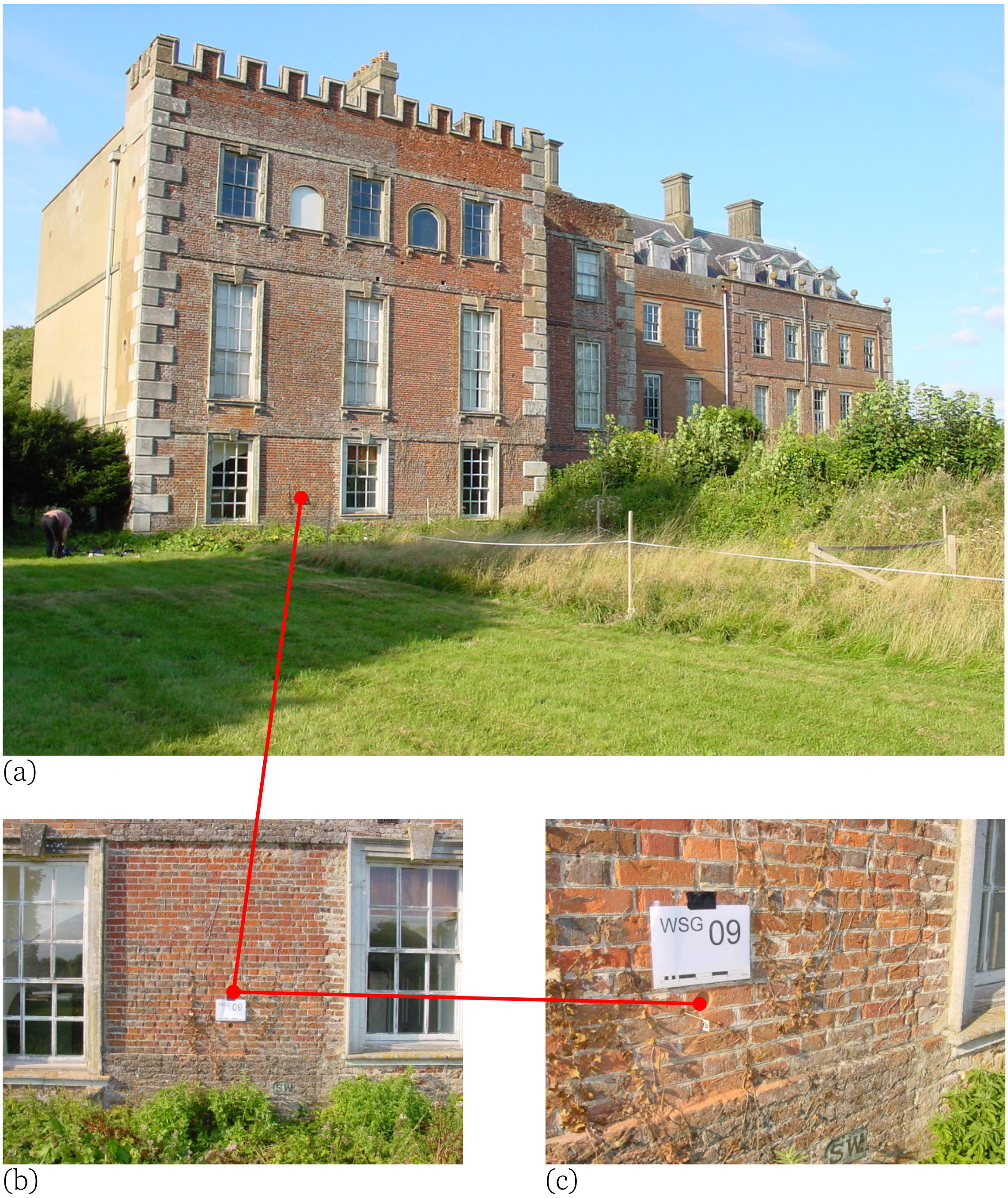

Figure 21: (a) south-facing wall of St Giles House with white card indicating location of WSG-09, (b) section of south-facing wall showing location of WSG-09, (c) close-up showing sampling location WSG-09 and dosemeter (flag D)

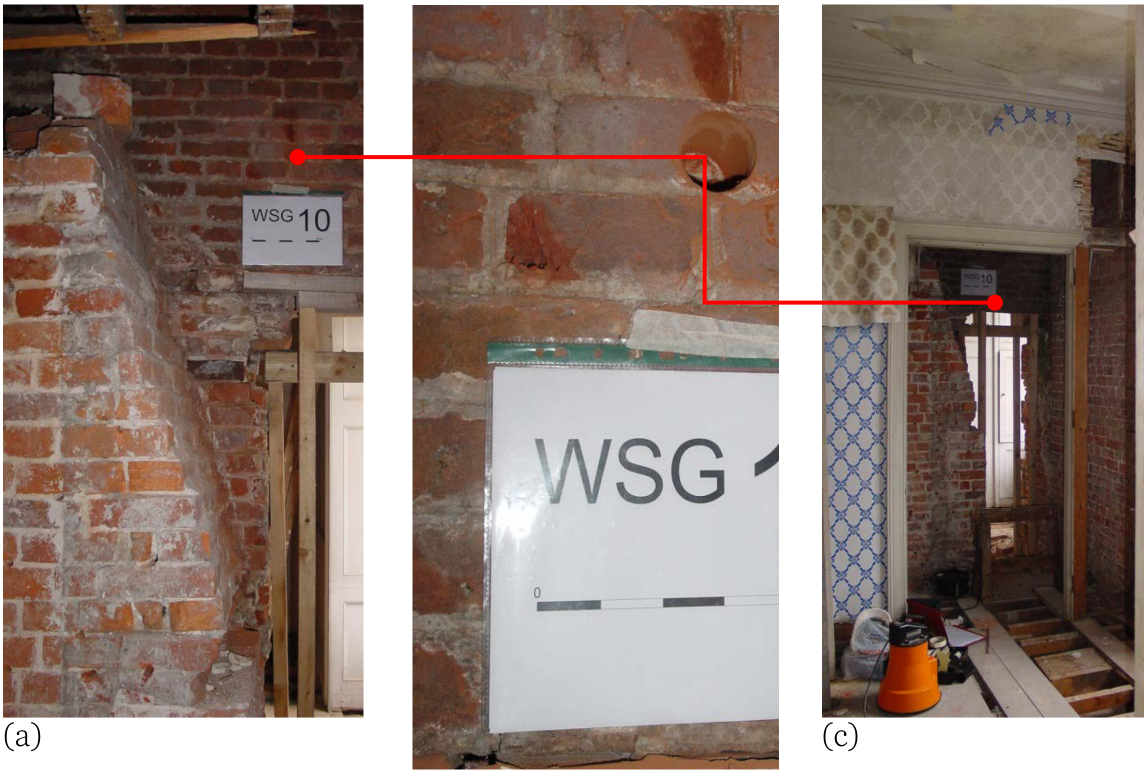

(a) (b) (c)

Figure 22: (a) north-facing interior wall on bedchamber floor adjacent to chimney stack in the Southampton Room, showing location of WSG-10, (b) close-up of sampling location WSG-10, (c) general view of location of WSG-10 in relation to west-facing exterior wall

(a) (b)

Figure 23: (a) location of WSG-11 in strong room where core is located four course above the white card in vaulted section, (b) close-up showing sampling location WSG-11 and dosemeter (circled)

(b)

(a)

Figure 24: (a) location of WSG-12, the core being located in the uppermost exposed brick, (b) close-up of sampling location WSG-12 showing core hole

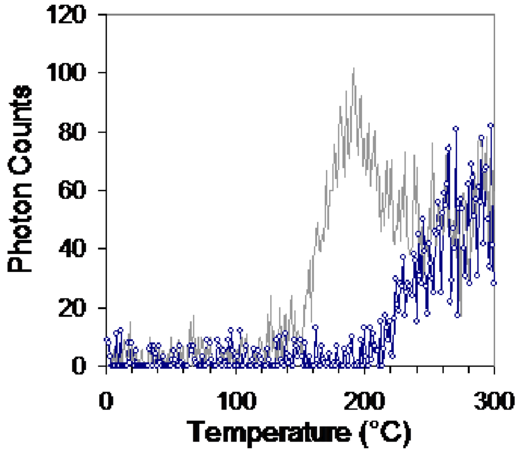

(a)

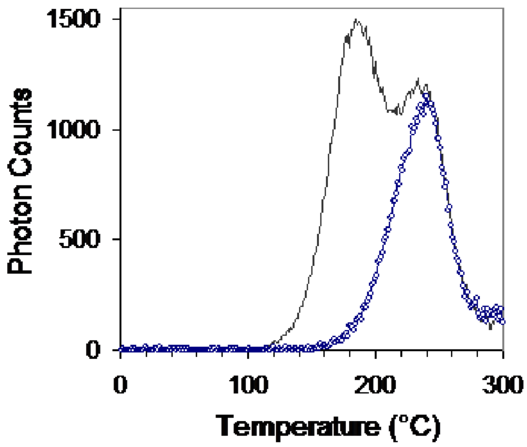

(b)

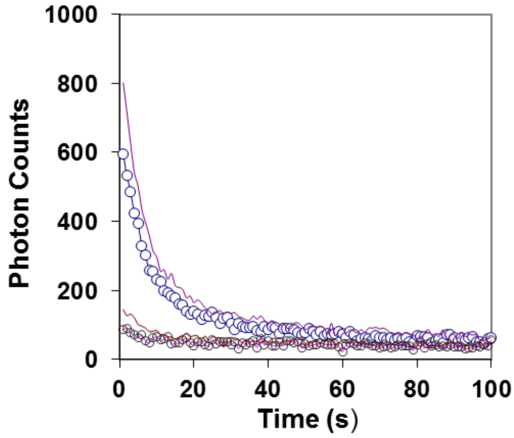

(c)

Figure 25: Examples of TL glow curves (a, b) and OSL decay curves (c) for different samples. Data points marked by open circles correspond to measurement of the 'natural' OSL or TL and the solid lines (no data point symbols) correspond to measurement following laboratory beta dose and pre-heating. The same symbol convention is applied to the pre-heat monitor OSL signals (c). The background TL signal has been subtracted in (a) and (b)

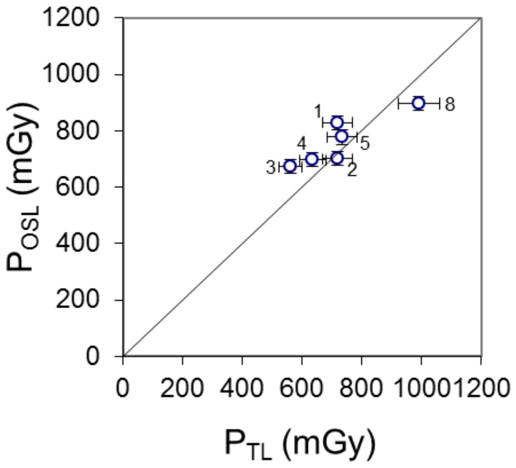

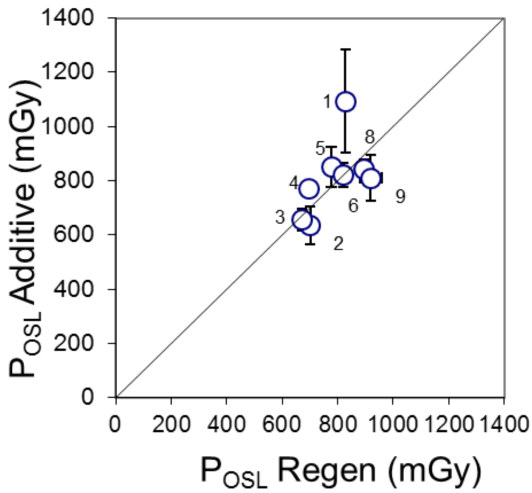

(a) (b)

Figure 26: Comparisons of P: (a) TL (210 °C TL peak) vs OSL (Regen), and (b) OSL (Regen) vs OSL (Additive Dose). Samples WSG01–WSG09 were tested. The line plotted in each figure represents a line of concordance

(a)

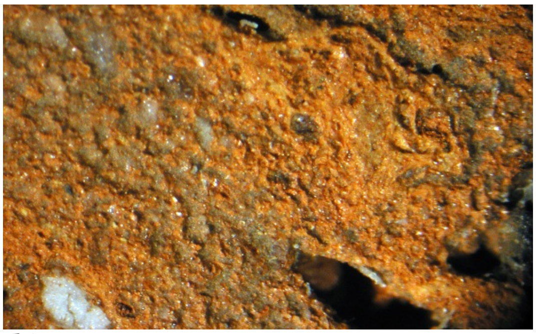

(b)

Figure 27: Images of brick core slice surface (WSG-07-2) showing (a) heterogeneity in brick composition and occurrence of fissures and (b) the clustering of crystalline inclusions (ie temper of diameter ~100–300μm) on left-hand side of image. Viewed under magnification of x16

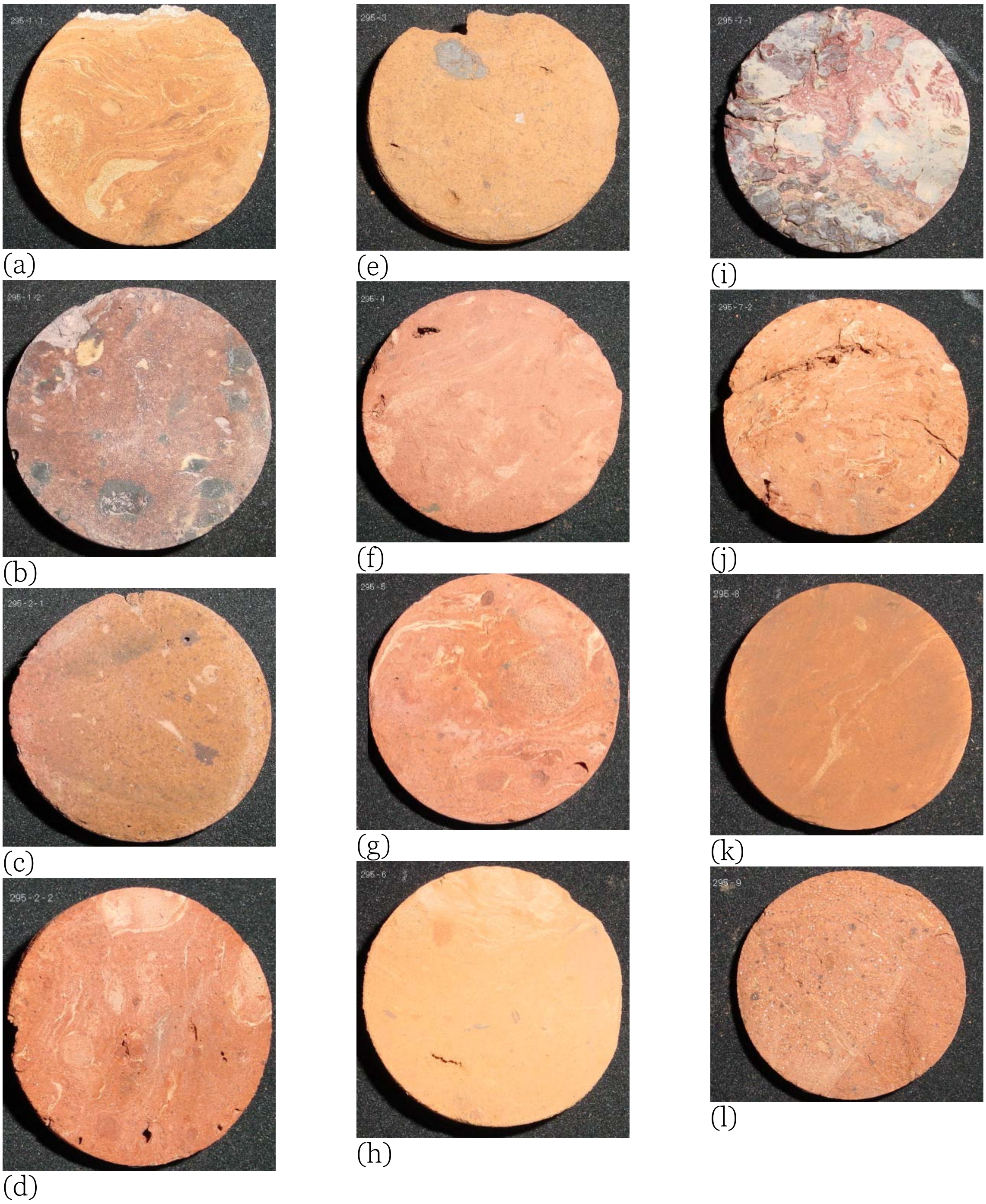

Figure 28: Images of sliced cores (core diameter ~50mm). (a) WSG-01-1, (b) WSG-01-2, (c) WSG-02-1, (d) WSG-02-2, (e) WSG-03, (f) WSG-04, (g) WSG-05, (h) WSG-06, (i) WSG-07-1, (j) WSG-07-2, (k) WSG-08, (l) WSG-09

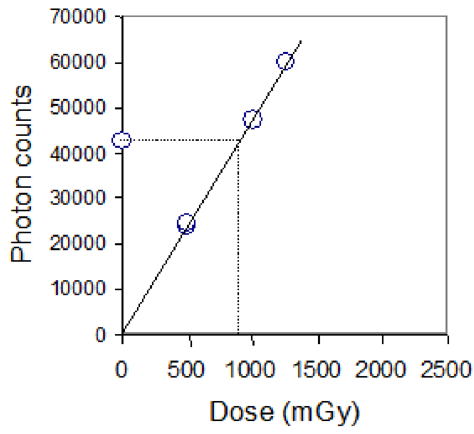

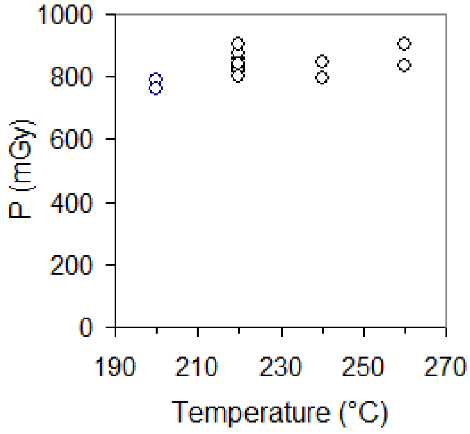

(a) (b)

Figure 29: Examples of (a) typical regenerative growth characteristic showing good linearity and (b) a plot of paleodose vs pre-heat temperature

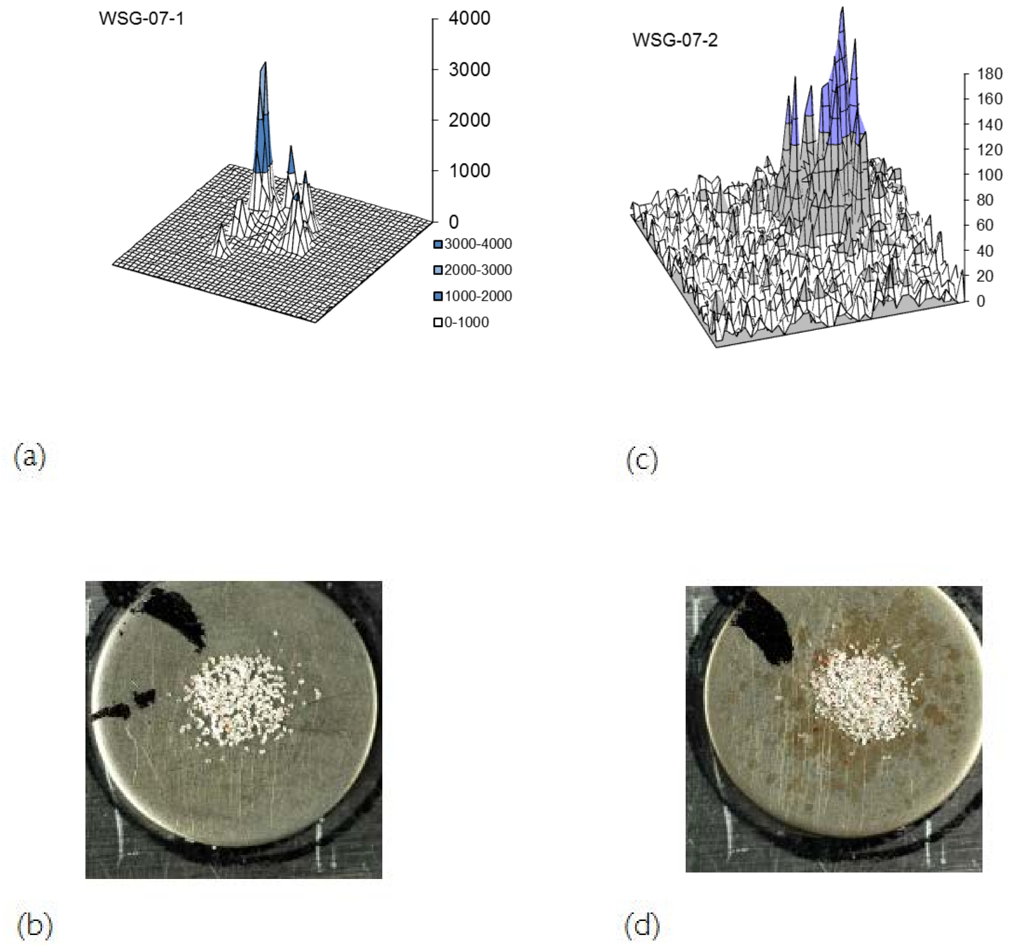

Figure 30: Spatially-resolved OSL (SROSL) from aliquots (~1–2 mg) of quartz grains placed on discs of ~9.5mm diameter: isometric views of intensity patterns following the administration of a beta dose where the scan area is ~10 x 10mm ((a) WSG-07-1, (c) WSG-07-2), and photographic images of the same aliquots showing the distribution of grains on the discs (plan views) ((b) WSG-07-1, (d) WSG-07-2). The SROSL for both WSG-07-1 and WSG-07-2 is heterogenous, and in the case of WSG-07-1 the pattern suggests a small number of very bright grains

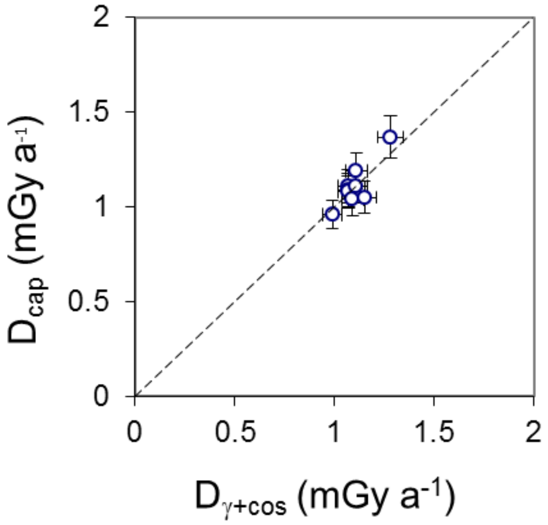

Figure 31: Comparison of the values of the combined gamma and cosmic annual dose at locations 1–9, obtained directly using dosemeters (D_{cap}) and indirectly ($D_{\gamma+cos}$) based on measurements of brick radioactivity, as discussed in the text. The line plotted represents a line of concordance

(a) (b)

Figure 32: Examples of backfilled core holes shortly after completion of sampling: (a) WSG-09, (b) WSG-03

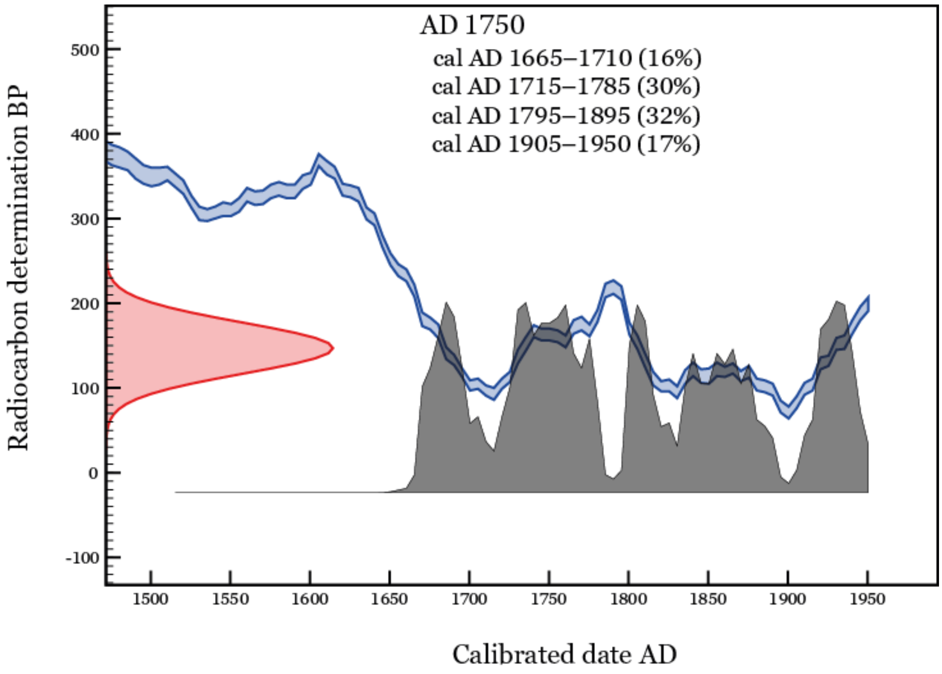

Figure 33: A simulated radiocarbon measurement for a sample with a calendar age of AD 1750 and an error on the radiocarbon measurement of ±30 years, in pink on the vertical axis, calibrated to cal AD 1665–1710 (16% probability), 1715–1785 (30% probability), 1795–1895 (32% probability) or 1905–1950 (17% probability), in black on the horizontal axis. The blue band is the relevant part of the calibration curve

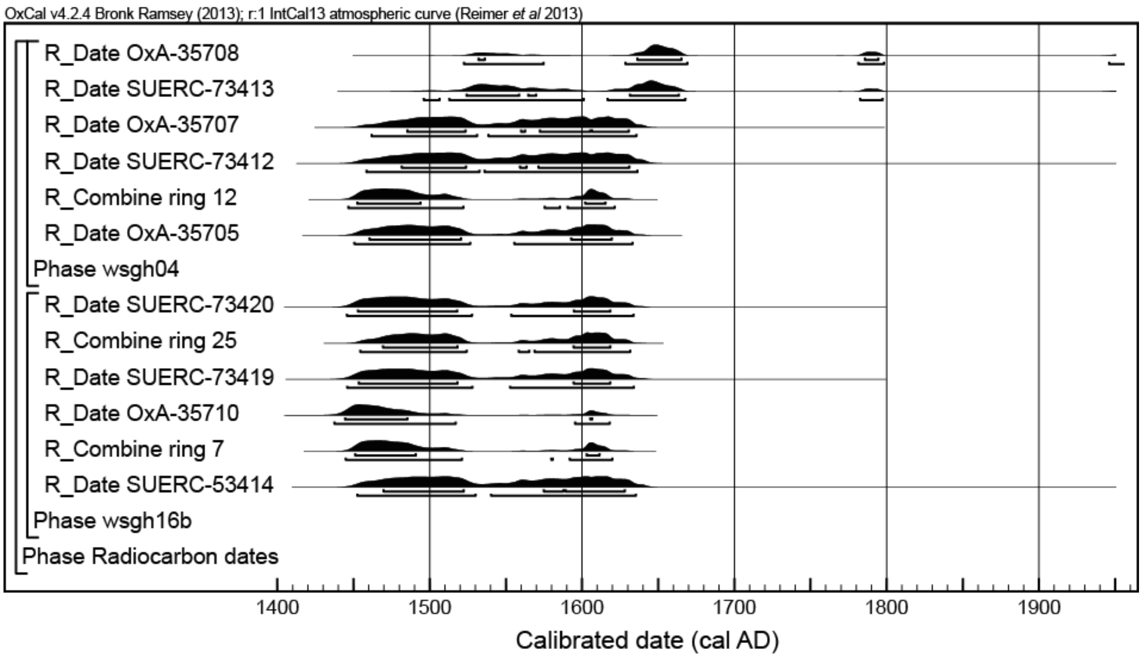

Figure 34: Calibrated radiocarbon dates from samples from timbers wsgh04 and wsgh16b (Stuiver and Reimer 1993)

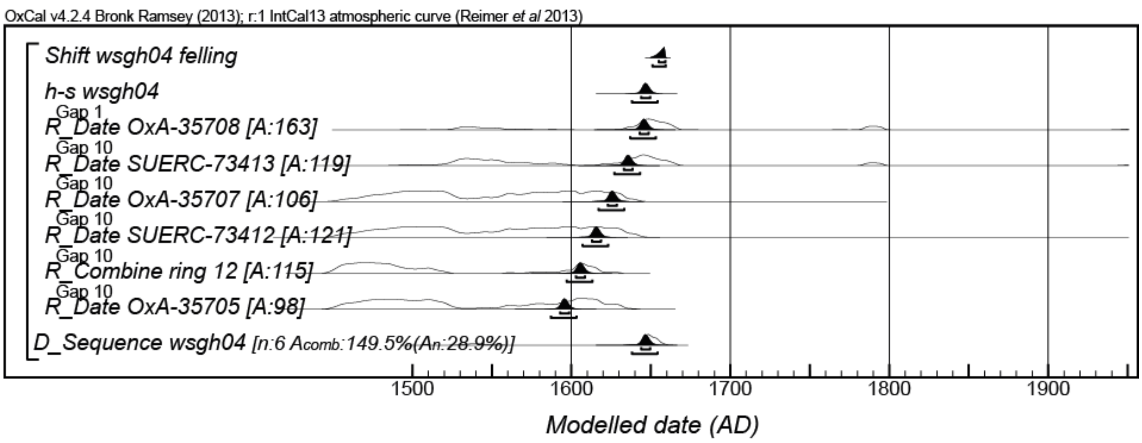

Figure 35: Probability distributions of dates from the timber wsgh04, from the ceiling in the former basement entrance hall. Each distribution represents the relative probability that an event occurs at a particular time. For each of the dates two distributions have been plotted: one in outline, which is the simple radiocarbon calibration, and a solid one, based on the wiggle-match sequence. The estimated date for the final ring is offset by the probability distribution of the expected number of sapwood rings on the timber (Miles 1997) to estimate the felling date of the timber. The large square brackets down the left-hand side along with the OxCal keywords define the overall model exactly

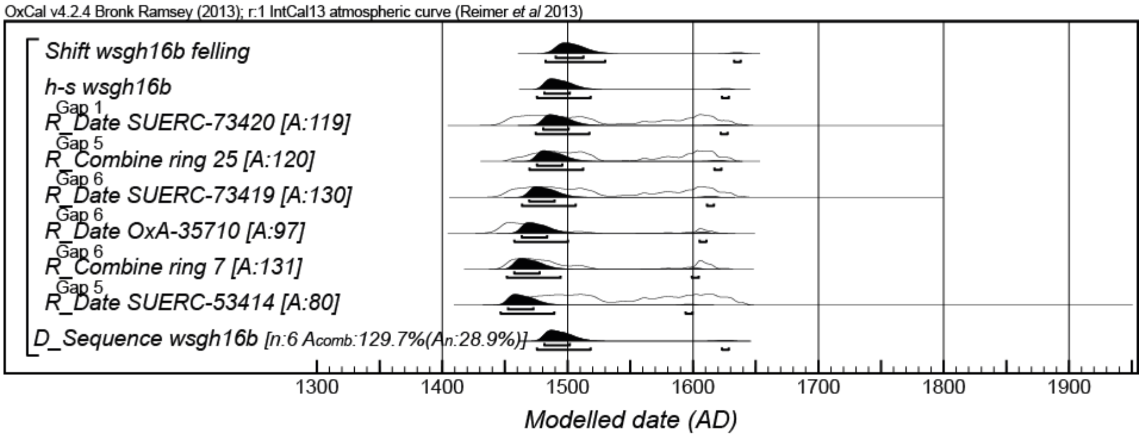

Figure 36: Probability distributions of dates from the timber wsgh16b, from the lintel above the fireplace in the kitchen. The format is as Figure 35. The large square brackets down the left-hand side along with the OxCal keywords define the overall model exactly

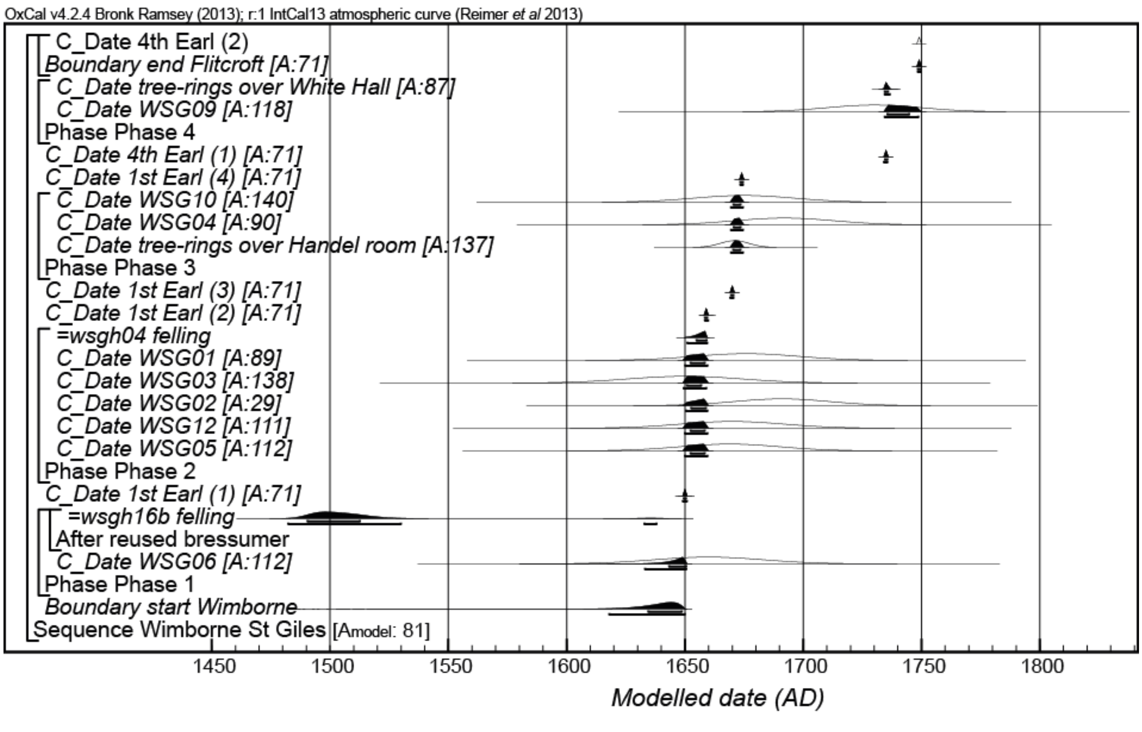

Figure 37: Probability distributions of scientific dates from St Giles House, incorporating the constructional sequence known from structural analysis and documentary evidence. The format is as Figure 35. The large square brackets down the left-hand side along with the OxCal keywords define the overall model exactly

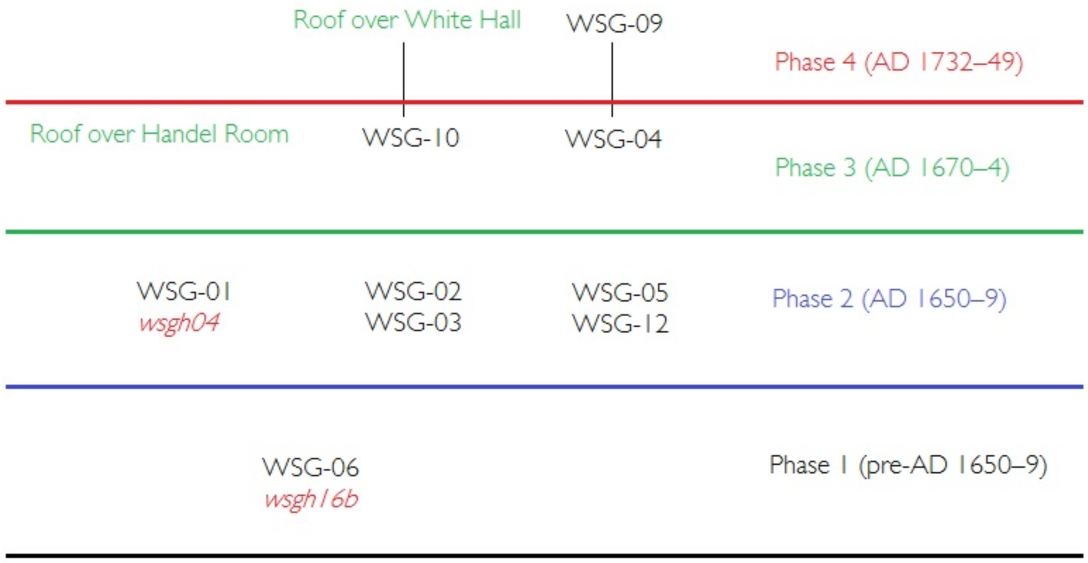

Figure 38: Diagram illustrating prior information derived from architectural, structural, and documentary evidence incorporated into the chronological model for St Giles House (black: luminescence ages; green: dendrochronology; red italic: radiocarbon wiggle-matching; solid lines indicate direct physical relationships between samples)

APPENDIX

Ring width values (0.01mm) for the sequences measured

wsgh01

273	205	376	602	380	546	406	438	537	553
380	507	315	213	157	252	341	332	365	320
317	416	441	368	377	266	348	277	263	220
294	286	334	164	252	275	154	172	147	185
219	305	239	231	203	231	223	230	171	119
142	183	251	300	202	207	229	223	195	162
117	135	170	202						

wsgh02

382	457	536	372	252	335	231	218	270	274
396	342	462	452	243	185	229	265	263	290
302	288	371	409	353	326	272	266	234	185
235	293	315	348	325	289	249	252	269	278
162	225	191	263	326	330	300	247	177	

wsgh04

194	362	313	410	275	344	306	287	418	414
356	329	252	340	329	377	293	294	245	201
317	264	305	336	289	332	350	276	335	306
289	230	234	216	212	161	235	208	178	225
171	144	148	240	251	282	339	261	336	243
186	180	283							

wsgh05

334	327	295	362	370	284	351	276	308	325
236	220	226	139	190	213	200	277	302	257
200	207	193	202	359	328	224	249	179	203
276	279	209	222	171	216	183	207	181	188
160	174	127	138	174	137	188	166		

wsgh07

223	214	375	205	353	374	272	276	244	282
187	354	350	286	215	237	258	180	159	203
225	207	174	164	176	222	237	244	233	265
329	201	217	293	268	136	165	120	165	177
192	234	236	91	121	116	165	168	85	158
143	126	135	192	162	155	188	169	195	186

wsgh08

329	360	301	385	270	254	232	209	231	258
259	307	283	253	339	339	384	299	302	226
193	179	194	193	186	172	180	241	253	313
260	315	183	204	140	159	129	182	224	301
268	327	244	200	266	280	320	377	321	286
227	194	177	202	248	224	198	243	183	143
200	219	269							

wsgh09

305	233	120	63	46	40	59	108	150	136
140	103	144	282	170	103	123	168	165	212
180	379	179	211	172	184	263	249	464	355
480	390	396	457	336	255	349	215	236	242
253	159	131	196	499	282	255	213	388	164
140	234	236	305	235	317	251	185	141	126
189	169	136	184	113	172	129	121	93	97
69	85	159	87	107	129	95	97	98	104
165	160	150	110	180	141	116	125	127	127
83	91	91	66	82					

wsgh10

216	178	176	176	266	220	190	164	215	137
116	146	155	174	154	181	213	176	146	164
156	129	133	156	150	171	153	158	117	148
110	115	142	125	135	131	114	125	99	102
127	134	149	141	157	120	128	132	138	146
123	133	127	102	93	92	107	145	81	93
88	92	107	98	113	95	79	119	129	126
90	111								

wsgh11

331	386	308	400	393	491	484	409	590	476
394	345	452	443	454	381	421	343	327	376
247	293	295	265	266	331	293	259	231	221
202	271	356	409	297	368	217	168	153	122
93	65	105	138	140	126	126	131	78	69
61	72	70	104	96	87	107	159	148	173
164	185	141	181	121	114	170	161	216	140
146	192	136	115	117	110	129	126	95	158
146	95	98	92	86	92	75	92	93	98
72	110	101	66	92	106	98	94	77	89

wsgh12

231	262	210	185	157	242	313	191	199	166
203	169	206	192	174	157	165	241	283	228
174	175	194	198	151	150	175	274	210	264
187	187	123	132	177	163	192	221	206	171
153	117	107	166	211	213	208	107	109	101
148	176	154	180	141	122	161	89	119	146
108	132	144	154	156	166	147	160	126	123
141	132	133	125	115	140	128	126	130	155
181									

wsgh13

477	427	420	448	424	427	367	429	401	389
325	306	231	241	343	323	302	336	352	392
280	277	274	303	266	248	284	232	309	317
288	315	271	286	275	161	164	150	156	231
185	200	203	193	156	139	156	153	146	187
136	132	139	129						

wsgh14

373	285	365	258	143	150	289	249	218	388
371	444	241	178	112	137	209	210	236	227
247	212	149	131	114	121	178	213	211	188
129	81	172	189	133	105	102	82	75	72
144	160	149	162	179	339	131	85	94	124
150	232	142	186	160	233	206	130	108	196
156	170	156	164						

wsgh15

266	287	243	212	191	208	205	187	231	256
256	249	301	237	292	273	227	242	207	91
149	209	198	164	191	159	203	153	155	124
159	206	219	190	169	187	151	173	134	125
150	208	175	163	162	144	78	143	164	107
87	106	96	103	100	118	120	124	99	97
113									

wsgh16a

353	484	441	233	373	573	417	398	493	524
482	382	244	217	280	243	298	254	253	297
221	157	166	176	200	231	323	382	333	275
266	239	266	279	140	139	200	257		

wsgh16b

167	139	185	196	312	288	350	362	273	417
282	272	240	261	296	185	202	155	277	259
250	243	256	282	303	283	331	248	252	204
272									

wsgr01

98	99	134	117	130	105	92	83	86	108
135	136	119	114	110	95	100	119	144	80
82	97	101	125	116	105	119	119	129	92
113	104	116	118	132	127	118	119	132	148
184	118	116	118	117	146	135	139	164	135
126	103	119	115	134	113	148	136	147	112
136	165	151	164	200	169	141	163	162	151
138	134	123	120	114	121	108	106	119	133
119	86	121	116	135	143	186	142	162	101
141	131	127	122	129	117	125	117	117	119
99	112	98	112	87	126	92	112	96	104
100	108	128	104	111					

wsgr02

424	482	567	530	489	513	291	178	375	396
370	496	467	407	342	332	212	166	201	319
206	243	319	204	163	133	122	184	238	202
197	266	192	162	154	210	193	175	136	191
178	227	109	140	142	179	186	174	162	169
169	181	125	107	188	222	144	174	195	202
175	193	275	183	133	127	115	129	137	210
202	183	137	84	97	60	93	96	171	205
243	187	181	206	250	309	296	262		

wsgr03

148	220	240	169	134	130	187	215	153	227
156	135	180	167	145	127	111	149	126	116
139	188	132	106	227	189	177	156	110	109
163	131	141	111	100	88	104	96	104	96
149	97	126	99	126	109	70	98	114	89
116	87	138	104	169	184	118	108	109	114
120	96	113	123	147	82	63	99	102	87
98	88	102	114	79	94	127	97	88	100
81	65	88	68	72	115	72	57	64	61
63	77	69	58	77	58	45	44	49	56
66	63	54	71	63	63	53	60	78	52
62	54	73	73	84	88	80	61	85	43
92	66	115	119	162	92	122	113	139	118
135	71	53	57	56	61	59	110	154	149
150	112	91	104	129	73	112	90	95	89
87	107	92	131	123	100	78	80	167	98
95	111	100	89	96	68	58	62	64	71
94	71	70	75	80	69	59	93	60	69
91	110	96	81	97	96	80	67	74	93
101	103	109	71	76	82	67	92	70	71
83	61	64	55						

wsgr04

295	191	197	301	444	369	470	455	351	397
299	332	255	175	195	214	264	271	292	336
385	320	536	257	136	169	168	148	187	257
321	347	309	310	186	169	146	217	138	153
187	234	305	268	364	240	92	84	51	109
139									

wsgr05

149	182	135	138	183	144	126	123	94	108
135	135	100	111	82	113	101	104	113	119
164	119	130	148	109	81	76	122	80	96
92	81	79	80	87	109	159	136	114	150
95	124	120	149	92	128	88	94	102	93
84	115	140	141	92	84	156	160	145	171
107	100	102	82	66	83	79	59	41	50
71	49	70	76	75	62	81	85	72	70
90	91	77	94	94	78	68	99	97	93
86	109	117	100	96	82	84	114	116	126
139	153	117	153	163	170	191	137	151	128

wsgr06

122	118	153	136	157	167	124	132	126	158
147	133	130	168	181	144	149	153	195	199
173	175	115	135	137	159	169	193	136	145
139	117	99	117	142	153	170	151	135	151
140	127	177	166	104	114	129	114	140	134
117	138	141	122	108	207	129	168	186	227
163	197	126	175	188	198	135	147	138	180
156	170	173	167	158	148	127	152	148	187
156	183	132	127	112	131	191	136	163	188
142	139	160	141	173	146	149	132	145	133
101	116	118	112	131	139	93	129	103	117
124	108	107	109	104	123	129	107	112	118
140									

wsgr07

171	450	402	151	126	198	212	255	198	142
209	122	99	180	221	364	305	227	167	322
264	93	180	126	194	175	163	178	171	178
152	228	135	177	222	166	122	118	162	115
170	119	184	186	164	187	167	267	143	170
119	110	103							

wsgr08

131	115	118	129	150	129	165	119	136	106
99	71	73	111	137	142	142	137	101	112
103	119	124	82	72	91	77	88	75	68
87	103	104	69	122	98	127	125	155	132
126	132	106	135	169	108	117	113	179	176
148	175	185	165	157	118	148	143	157	136
158	126	138	125	136	167	134	149	157	146
135	132	131	144	152	123	122	103	109	107
124	102	128	122	99	103	107	114	133	133
144	125	165	123	118	121	128	127	130	126
117	99	110	103	96	117	129	113	108	103
90	94	101	104	140	128	109	147		

wsgr09

321	388	580	487	466	592	410	526	421	511
340	386	369	298	309	240	391	345	296	283
272	295	323	261	198	243	243	251	159	190
185	136	153	180	122	148	158	225	219	206
177	147	125	125	95	93	95	102	110	95
118	113	125	142	97	84	76	58	57	65
62	59	59	50	57	57	51	83	85	109
136	134	80	82						

wsgr10

259	262	159	189	189	222	295	245	238	317
304	269	210	244	230	177	256	228	202	181
169	208	192	231	223	240	262	199	325	285
215	253	189	219	162	186	179	234	208	286
171	202	159	113	105	170	131	158	155	196
189	175	189	151	137	95	133	132	111	144
120	120	133	91	69	110	130	95	122	78
125									






Historic England Research and the Historic Environment

We are the public body that looks after England's historic environment. We champion historic places, helping people understand, value and care for them.

A good understanding of the historic environment is fundamental to ensuring people appreciate and enjoy their heritage and provides the essential first step towards its effective protection.

Historic England works to improve care, understanding and public enjoyment of the historic environment. We undertake and sponsor authoritative research. We develop new approaches to interpreting and protecting heritage and provide high quality expert advice and training.

We make the results of our work available through the Historic England Research Report Series, and through journal publications and monographs. Our online magazine Historic England Research which appears twice a year, aims to keep our partners within and outside Historic England up-to-date with our projects and activities.

A full list of Research Reports, with abstracts and information on how to obtain copies, may be found on www.HistoricEngland.org.uk/researchreports

Some of these reports are interim reports, making the results of specialist investigations available in advance of full publication. They are not usually subject to external refereeing, and their conclusions may sometimes have to be modified in the light of information not available at the time of the investigation.

Where no final project report is available, you should consult the author before citing these reports in any publication. Opinions expressed in these reports are those of the author(s) and are not necessarily those of Historic England.

The Research Report Series incorporates reports by the expert teams within the Research Group of Historic England, alongside contributions from other parts of the organisation. It replaces the former Centre for Archaeology Reports Series, the Archaeological Investigation Report Series, the Architectural Investigation Report Series, and the Research Department Report Series

ISSN 2398-3841 (Print)
ISSN 2059-4453 (Online)